Ore Geology Reviews 90 (2017) 193–209

Contents lists available at ScienceDirect

Ore Geology Reviews

journal homepage: www.elsevier.com/locate/oregeo

Zircon recycling and crystallization during formation of chromite- and Ni-arsenide ores in the subcontinental lithospheric mantle (Serranía de Ronda, Spain)

José M. González-Jiménez [a,b,c,*], Claudio Marchesi [a,d], William L. Griffin [c], Fernando Gervilla [a,d], Elena A. Belousova [c], Carlos J. Garrido [d], Rurik Romero [b], Cristina Talavera [e], Mathieu Leisen [b], Suzanne Y. O'Reilly [c], Fernando Barra [b], Laure Martin [f]

[a] Departamento de Mineralogía y Petrología, Universidad de Granada, Facultad de Ciencias, Fuentenueva s/n 18002, Granada, Spain
[b] Department of Geology and Andean Geothermal Center of Excellence (CEGA), FCFM, Universidad de Chile, Plaza Ercilla 803, Santiago, Chile
[c] ARC Centre of Excellence for Core to Crust Fluid Systems (CCFS), and GEMOC National Key Centre, Department of Earth and Planetary Sciences, Macquarie University, Sydney, NSW 2109, Australia
[d] Instituto Andaluz de Ciencias de la Tierra (IACT), CSIC-UGR, Avda. de las Palmeras 4, 18100 Armilla, Granada, Spain
[e] Department of Physics and Astronomy, Curtin University, Perth, WA 6102, Australia
[f] Centre for Microscopy Characterisation and Analysis, The University of Western Australia, Crawley, WA 6009, Australia

ARTICLE INFO

Article history:
Received 21 June 2016
Received in revised form 6 February 2017
Accepted 8 February 2017
Available online 15 February 2017

Keywords:
Chromite-Ni arsenide ores
Mantle metasomatism
Zircon
Lithospheric mantle
Crustal recycling

ABSTRACT

The ultramafic massifs of the Serranía de Ronda (namely Ronda, Ojén and Carratraca) are portions of Proterozoic (~1.2–1.8 Ga) subcontinental lithospheric mantle (SCLM) affected by partial melting and infiltration of melts. The latter of these events was broadly coeval with the tectonic emplacement of the peridotites into the continental crust in the Early Miocene. This resulted in the formation of chromite and Ni-arsenide ores (Cr-Ni) associated with orthopyroxenites and cordieritites. Six zircons recovered from a massive chromitite sample from the Ronda massif yield both concordant and discordant ages between 2309 ± 37 Ma and 109 ± 15 Ma, and $\delta^{18}O$ between 8.3‰ and 9.4‰. Two Proterozoic ages obtained for zircons of this population (1815 ± 9 Ma and 1794 ± 17 Ma) are identical, within error, to those of zircons reported previously in the garnet pyroxenites of Ronda (1783 ± 37 Ma). Similarly, concordant Early Jurassic (192 ± 13 Ma) and Cretaceous ages (109 ± 15 Ma) obtained from the core and rim, respectively, of a single zircon from the chromitite are also consistent with the ages (180 ± 5 Ma, 178 ± 6 Ma, and 131 ± 3 Ma) already reported for magmatic zircons from corunudum-bearing garnet pyroxenites in the Ronda massif. The observation that chromitites and garnet-pyroxenites contain similar populations of zircons suggests that the parental melts of chromitites inherited zircons from their protolithic garnet pyroxenites, representing relics of oceanic/arc crust recycled in the mantle. Eleven zircons recovered from a massive cordieritite associated with chromitite in the Ronda massif yield scattered concordant and discordant ages between 568 Ma and 21 Ma, with correspondingly variable $\delta^{18}O$ (4.8–13.5‰) and unradiogenic Hf-isotope ratios ($\varepsilon_{Hf}(t)$ from −12.36 to −4.43). The youngest age is concordant at 21.18 ± 0.4 Ma and matches the ages of zircons from the chromitite (weighted average age of 20.4 ± 0.87 Ma, n = 4) and a plagioclasite dyke (scattering between 20.1 ± 0.2 Ma and 17.9 ± 0.1 Ma; n = 11) associated with the Cr-Ni mineralization in the Ojén massif. These zircons show similar unradiogenic Hf-($\varepsilon_{Hf}(t)$ between −14.5 and −7.6) and heavy O-isotope compositions ($\delta^{18}O$ = 11.3–12.4‰). A sample of the massive cordieritite hosting the chromitites contains abundant zircons that yield scattered concordant, sub-concordant and discordant U-Pb ages varying from 33.8 ± 1 Ma to 781 ± 10 Ma; these zircons (n = 21) have variable U-contents (105–13900 ppm) and Th/U ratios (0.003–0.8). On the basis of O- and Hf-isotope compositions, these zircons define three populations independently of their ages: (1) grains with consistent high $\delta^{18}O$ (6.1–12.7‰) and negative $\varepsilon_{Hf}(t)$ (from −14.42 to −6.88); (2) grains with high $\delta^{18}O$ (7.6–11.1‰) and positive $\varepsilon_{Hf}(t)$ (3.10–4.84); and (3) grains with $\delta^{18}O$ < 5.5‰ typical of mantle values. We suggest that zircons from this cordieritite with U-Pb ages older than Miocene are inherited, and were incorporated physically into the SCLM by fluids or melts produced during dehydration-melting of the crustal rocks wrapping the peridotite massifs. The population of Early Miocene zircons found in the chromitites and associated cordieritites and the plagioclasite dyke in the

* Corresponding author at: Universidad de Chile, Departamento de Geología, Plaza Ercilla # 803, Santiago de Chile, Chile.
E-mail address: jmgonzj@ing.uchile.cl (J.M. González-Jiménez).

http://dx.doi.org/10.1016/j.oregeorev.2017.02.012

mineralization of the Ojén massif date the crustal emplacement of the peridotites and, therefore, the formation of the Cr-Ni ores. We propose a model in which the unique Cr-Ni mineralizations found in the ultramafic rocks of the Serranía de Ronda were formed as a result of contamination of the SCLM with crustal components.

1. Introduction

Zircon ($ZrSiO_4$) is a common accessory mineral in many types of rocks. *In situ* data for a suite of radiogenic (U-Th-Pb, Lu-Hf, Sm-Nd) and stable isotopes (O), which can be obtained from single zircon grains (Griffin et al., 2002, 2004; Kinny and Mass, 2003; Valley, 2003; Valley et al., 2005; Belousova et al., 2010), make this mineral an unmatched tool to study the formation of the early Earth (Cavosie et al., 2007; Harrison, 2009; Marchi et al., 2014) and the construction and recycling of continents and oceans during orogenic episodes (Condie et al., 2009; Belousova et al., 2009, 2010). Zircon can also be used to constrain different types of geological processes that involve fluids or melts, such as hydrothermal alteration, metamorphism and remelting of igneous bodies (Belousova et al., 2002; Hoskin and Schaltegger, 2003). Over decades, most efforts have been focused on the study of zircons from crustal domains, in which this mineral is most frequently found. In the mantle, however, the study of zircon has received less attention, as peridotites are generally depleted in Zr and Si, and the melts extracted from these rocks are theoretically not likely to precipitate zircons. In recent years, however, an ever-increasing number of studies have reported zircons in different suites of mantle rocks, including peridotites (Bea et al., 2001; Hermann et al., 2006; Zheng et al., 2006; Zheng, 2012), pyroxenites (Gebauer, 1996; Sanchez-Rodriguez and Gebauer, 2000) and chromitites (Grieco et al., 2001; Yamamoto et al., 2003, 2004, 2013; McGowan et al., 2015; González-Jiménez et al., 2015; Xu et al., 2015; Xiong et al., 2015; Belousova et al., 2015; Akbulut et al., 2016; Griffin et al., 2016; Li et al., 2016). In the aforementioned works, interpretations of zircons from the mantle vary between the hypotheses that these minerals crystallize in the mantle itself (i.e., they are *metasomatic*), or that zircons were formed in the crust and recycled in the mantle by subduction or delamination of the continental crust. Unravelling the origin of zircons in mantle-derived rocks might help to better understand the exchange of material between distinct layers of the solid Earth (Siebel et al., 2009 and Liou and Tsujimori, 2013 for review), and in particular the genesis of chromite ores in the upper mantle.

Chromitites hosted in the mantle section of some ophiolites (e.g., the Luobusa and Dongqiao ophiolites in Tibet) preserve zircons (Zhou et al., 2014; Robinson et al., 2015; Xu et al., 2015; McGowan et al., 2015; Xiong et al., 2015) that coexist with minerals typical of ultra-high pressure (UHP $\geq$ 4 GPa; diamond, TiO_2 II, coesite, and stishovite pseudomorphs) and super-reducing conditions (native elements, alloys, carbides, nitrides), forming the so-called SuR-UHP (Super-Reduced UHP) assemblage (Griffin et al., 2013, 2016). This assemblage in chromitites has been interpreted to reflect mechanical entrapment of minerals by asthenospheric melts generated at >150 km (Zhou et al., 2014; Robinson et al., 2015) that assimilated crustal material (including zircon) during upwelling through slab windows in the lithosphere, or mineral entrapment by plume melts from greater depths (>420–660 km) which rose through the mantle transition zone that contains stagnant lithospheric slabs (Xu et al., 2015; Xiong et al., 2015). Both models require the crystallization of chromitites at high pressures (>13 GPa) from high-Mg melts similar to komatiites, and their later transport in a melt or fluid phase. However, this is a very unlikely scenario for chromite, which, according to experimental data, crystallizes at much lower pressures (<1 GPa; Sen and Presnall, 1984) from basaltic melts relatively rich in CaO and SiO_2 (Hill and Roeder, 1974; Ballhaus, 1998). In addition, chromite is too dense to be transported over >400 km by rising fluids/melts (Griffin et al., 2016). On the other hand, (magmatic and inherited) zircon populations in chromitite and host peridotites from the Coolac Serpentinite Belt in SE Australia yield U-Pb ages and geochemical fingerprints coincident with those of the surrounding S-type granites (Belousova et al., 2015). A similar situation was observed in the Oman ophiolite (Yamamoto et al., 2013) and some Tibetan Ophiolites (Griffin et al., 2016) where some zircons in the mantle-hosted chromitites yield U-Pb ages younger than the accepted age of crustal emplacement of the ophiolite. These observations suggest that mantle rocks may also experience zircon incorporation from neighboring rocks during or after their emplacement into the crust.

The examples cited above show that, despite numerous and detailed studies, the origin of zircons in mantle rocks is still open to debate. In particular, the role of crustal metasomatism in the formation and incorporation of zircons in the subcontinental lithospheric mantle (SCLM) and its relationships to the genesis of chromite ores are still uncertain. In this paper, we report the discovery of zircons in the chromite- and Ni-arsenide ores [hereafter (Cr-Ni)-cordierite ores] hosted in the ultramafic massifs of the Serranía de Ronda (S. Spain), the largest outcrops of SCLM exposed on the Earth's surface. Recent geochemical studies (Marchesi et al., 2012; Varas-Reus et al., 2016) indicate that melts/fluids derived from underthrusted metasedimentary rocks infiltrated the Ronda peridotites shortly before or during their crustal emplacement, producing crustal metasomatism of the SCLM. Interestingly one $^{40}Ar/^{39}Ar$ age on primary phlogopite from a plagioclasite associated with one of the Ronda's (Cr-Ni)-cordierite mineralization yield an Aquitanian age (Gervilla and Leblanc, 1990) that matches with the time of this metasomatism of the peridotites by crustal melts/fluids. This scenario gives us the opportunity to evaluate how crustal fluids/melts may form or incorporate zircons in the SCLM, as well as the impact of these processes in the formation of chromitites in the upper mantle. Using the most innovative techniques of mineral separation (Selfrag) we have recovered zircons from all types of rocks that form these ores, namely massive chromitites (some of them anomalously rich in Ni-arsenides), cordieritites and associated plagioclasite dykes. We have measured *in situ* a suite of radiogenic (U-Pb, Lu-Hf) and stable isotopes (O) on zircons in order to constrain the age and nature of the parental fluids/melts from which they crystallized. We integrate these zircon data with the most recent geochemical, petrological and structural data in order to build a new model for the genesis and evolution of the Ronda's chromite ores.

2. Geological background

2.1. The ultramafic massifs of the Serranía de Ronda

The ultramafic massifs of the Serranía de Ronda crop out in the westernmost part of the Internal Zones of the Betic-Rif orogenic belt, namely the westernmost branch of the Mediterranean Alpine belt (Fig. 1). The Internal Zones are composed of three nappe complexes that have variable metamorphic grades and are, from bot-

tom to top: the Nevado-Filábride, Alpujárride and Maláguide Complexes. The peridotites of the Serranía de Ronda form the lowest part of the Los Reales Nappe, the uppermost tectonic unit of the Alpujárride Complex, and are sandwiched between continental crustal rocks (Navarro-Vilá and Tubía, 1983; Tubía and Cuevas, 1986). These ultramafic rocks crop out in three separate massifs (Fig. 1): Ronda (considered the largest (~300 km^2) exposure of continental mantle peridotite on Earth), Ojén (~ 80 km^2), and Carratraca. These peridotite massifs represent portions of Proterozoic (1.2–1.8 Ga) subcontinental lithospheric mantle (Reisberg and Lorand, 1995; Marchesi et al., 2010; González-Jiménez et al., 2013a,b) emplaced tectonically into the crust in the Early Miocene (Zindler et al., 1983; Zeck et al., 1989; Monié et al., 1994; Platt et al., 1998; Sanchez-Rodriguez and Gebauer, 2000; Esteban et al., 2004, 2007, 2010; Precigout et al., 2007), probably during the development of a back-arc basin behind the Betic-Rif orogenic wedge (Garrido et al., 2011; Marchesi et al., 2012; Hidas et al., 2013, 2015). Within the Los Reales Nappe, the ultramafic rocks are overlain by a thick (up to 7 km) sequence of metapelitic rocks that show decreasing metamorphic grade outwards from the contact with the peridotites (i.e., from acidic granulites (kinzigites), gneisses and migmatites, to schists, phyllites and, locally, marbles; Balanyá et al., 1997; Tubía et al., 1997; Platt et al., 2013), and are thrust over a carbonate-rich metasedimentary unit that contains relatively abundant bodies of amphibolite (Tubía et al., 1997; Sanchez-Rodriguez and Gebauer, 2000; Acosta-Vigil et al., 2014).

The ultramafic massifs of the Serranía de Ronda mainly consist of lherzolites and harzburgites with minor dunites and different

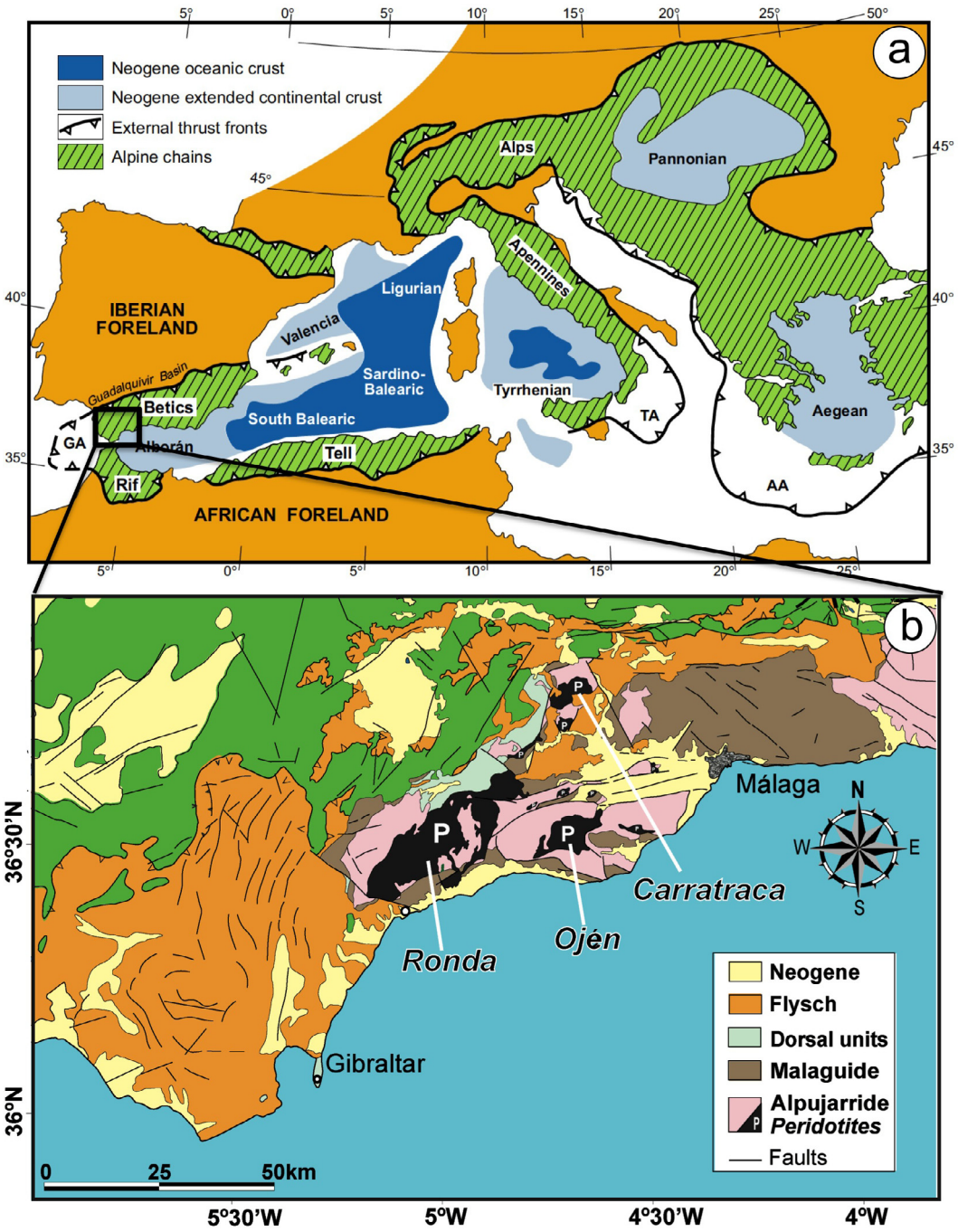

Fig. 1. (a) Localization of the Betic Belt within the Alpine orogeny and (b) outcrops of peridotite massifs in the western Betics.

types of pyroxenite layers, which are locally intruded by leucocratic dykes. A great body of work published over the past three decades, especially focusing on the Ronda peridotites, provides the basis to distinguish four kilometre-scale, structural, petrological and geochemical domains from top to bottom of the mantle section (Fig. 2): (1) *garnet mylonite domain*, (2) *spinel tectonite domain*, (3) *granular peridotite domain*, and (4) *plagioclase tectonite domain*.

The *garnet mylonite domain* (missing in the Ojén and Carratraca massifs) is in direct contact with the granulitic crustal units in the NW boundary of the Ronda massif, and it is in contact to the southeast with foliated *spinel tectonites* locally intercalated with garnet pyroxenites (Fig. 2). These domains represent vestiges of an old Proterozoic subcontinental lithospheric mantle with a protracted record of early exhumation from the roots of thick continental lithosphere in the diamond facies (Davies et al., 1993) and final emplacement in an extremely attenuated shallow continental lithosphere in the Miocene (Garrido et al., 2011; Hidas et al., 2013).

The *coarse granular peridotite domain* is located in the central part of the ultramafic bodies (Fig. 2), and is separated from the spinel tectonites by a narrow (~200 m wide) "recrystallization front" (Van der Wal and Vissers, 1993; Van der Wal and Bodinier, 1996). The granular peridotites were produced at the expense of precursor spinel tectonites during asthenospheric upwelling related to extension in the Late Oligocene. The latter tectonic event caused heating of the thinned lithospheric mantle at ~1.5 GPa and ≥1200 °C and melting of Ronda garnet pyroxenites and peridotites, producing km-scale infiltration of mafic and calcalkaline volatile-rich melts (Van der Wal and Bodinier, 1996; Garrido and Bodinier, 1999; Lenoir et al., 2001; Bodinier et al., 2008; Marchesi et al., 2012). Close to the recrystallization front, melt/rock reaction mainly led to the coarsening of the constituent minerals and precipitation of secondary clinpyroxene and sulfides, producing refertilized lherzolites and spinel websterites (Garrido and Bodinier, 1999; Lenoir et al., 2001; Bodinier et al., 2008; Marchesi et al., 2013, 2014). Therefore, the recrystallization front first defined by Van der Wal and Vissers (1993) can be considered as the frozen boundary between the old Proterozoic subcontinental lithospheric mantle (the spinel tectonite and garnet mylonite domains) and a mantle region fluxed by partial melts generated by Late Oligocene asthenospheric upwelling (Lenoir et al., 2001). Partial melts extracted from the granular peridotites locally crossed the recrystallization front and segregated residual, volatile-rich small-volume melts with boninitic affinity that formed discordant dykes of chromium-rich websterite (Van der Wal and Bodinier, 1996; Garrido and Bodinier, 1999; Marchesi et al., 2012).

The *plagioclase tectonite* domain is superimposed on the granular peridotites by the development of ductile deformation that overprinted most of the magmatic features described above. This deformation was produced during decompression (<1 GPa) and cooling of the massifs, and was concentrated along discrete shear-zones and folds that controlled the intracrustal emplacement of peridotites (Van der Wal and Vissers 1993, 1996; Esteban et al., 2010; Hidas et al., 2013).

Leucocratic dykes and pods, usually less than ten meters thick, intrude the Ronda peridotites through late sets of open cracks, especially in areas close to the country rocks (Hernández-Pacheco, 1967; Cuevas et al., 2006). These leucocratic dykes and pods have a wide range of compositions (i.e., granite, granodiorite, monzonite and transitional rocks between these end-members), and they are interpreted to have been generated by partial melting of the underlying migmatites during the emplacement of the hot ultramafic rocks into the crust (Sánchez-Rodriguez and Gebauer, 2000; Pereira et al., 2003; Cuevas et al., 2006; Esteban et al., 2007, 2010). Most of these dikes are undeformed and yield crystallization ages between 22 and 19 Ma, although some were folded during the latest ductile deformation.

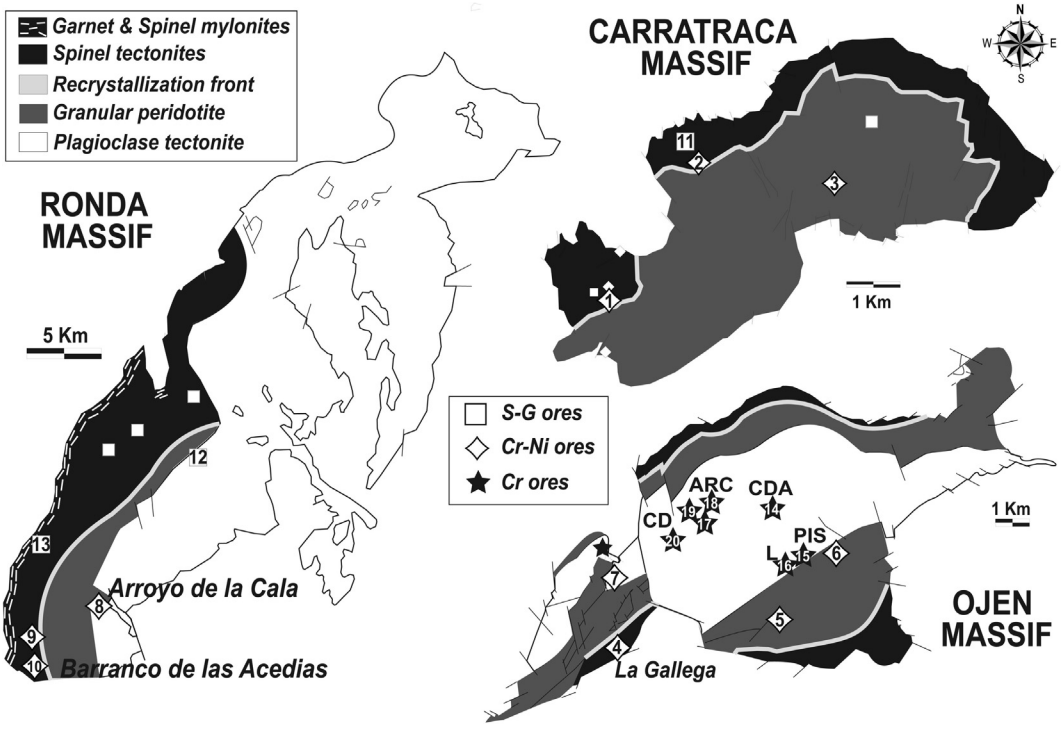

Fig. 2. Petro-structural zoning of the ultramafic massif of the Serranía de Ronda and distribution of the different magmatic ores. Cr-Ni ores: 1: Los Jarales district; 2: San Agustín; 3: El Sapo; 4: La Gallega; 5: El Lentisco; 6: El Nebral; 7: Mina Baeza; 8: Arroyo de la Cala; 9: Majada Redonda; 10: Barranco de las Acedías. S-G ores: 11: El Gallego; 12: Mina Marbella; 13: Arroyo de la Cueva. Cr ores: 14: Cerro del Águila (CDA); 15: Pista (PIS); 16: Lentisco (L); 17–19: Arroyo de los Caballos (ARC); 20: Cantera de Dunitas (CD).

2.2. The magmatic ores of the Serranía de Ronda ultramafic massifs

From a metallogenic point of view, the ultramafic massifs of the Serranía de Ronda are characterized by the occurrence of different types of magmatic Cr, Ni, Cu and platinum-group element (PGE) ores (Oen, 1973; Gervilla and Leblanc, 1990; Gervilla et al., 1996; Gutiérrez-Narbona et al., 2003; Crespo et al., 2006; González-Jiménez et al., 2013b), which are classified into three groups (Gervilla and Leblanc, 1990): (1) *sulfide-graphite (S-G) ores*, (2) *chromium (Cr) ores*, and (3) *chromium-nickel (Cr-Ni) ores*. This assemblage of magmatic ores is unique in the world and is distributed according to the petrological-structural domains of the ultramafic massifs (Fig. 2).

S-G ores constitute veins, stockworks and irregular masses of massive ore of variable size. Most deposits are a few meters in length and few centimeters thick, although some of the largest deposits (which were mined in the past) were up to tens of meters in lateral extension. These veins frequently contain xenoliths of the host rocks (peridotites and pyroxenites) and, locally, exhibit brecciated textures. In the S-poor occurrences, weathering transformed the original sulfides into earthy masses of Fe oxi-hydroxides containing irregular to round graphite concentrations (up to 90% in volume; Crespo et al., 2006). In the unaltered ores, the primary mineralogy is preserved and mainly consists of Fe-Ni-Cu sulfides (pyrrhotite, pentlandite, chalcopyrite and cubanite), chromite and graphite (10–60% in volume). Accessory minerals include rutile, bravoite, magnetite, maucherite, mackinawite and cobaltite (Gervilla and Leblanc, 1990). Leblanc et al. (1990) showed that unaltered *S-G* ores contain appreciable amounts of PGEs (218–800 ppb) and gold (13–230 ppm). These ores are associated with late fault zones within the spinel tectonite domain or close to the recrystallization front in the granular peridotite domain (Fig. 2). Gervilla et al. (2000) showed that PGE occur both as rare dispersed platinum-group minerals (koltuskite [Pd(Te,Bi)], froodite [$PdBi_2$] and palladian melonite [$(Ni,Pd)Te_2$]), and in solid solution in nickel arsenides (Pd contents up to 70 ppm and 103 ppm in nickeline and maucherite, respectively; Piña et al., 2013) and to a lesser extent in sulfides (usually at sub ppm levels but pentlandite contains up to 3.9 ppm Pd; Piña et al., 2013).

Cr ores are pods, lenses, irregular and entwined veins or schlieren of chromite enclosed in tabular dunites hosted in lherzolites and harzburgites of the plagioclase tectonite domain (Fig. 2). These chromite bodies are small (5 m in length and up to 30 cm in thickness) and often contain slices or lenses of Cr-rich pyroxenites (both Type D clinopyroxenites and orthopyroxenites of Garrido and Bodinier, 1999). *Cr ores* are relatively enriched in Os-rich platinum-group minerals (Torres-Ruíz et al., 1996; Gervilla et al., 1999; Gutierrez-Narbona et al., 2003), which have Os isotopic signatures typical of mantle sources (González-Jiménez et al., 2013b). The magmatic textures of the chromitite bodies, their morphology, composition, PGM assemblages and silicate inclusions resemble those of chromitites hosted in ophiolites (González-Jiménez et al., 2014).

Cr-Ni ores are made up of chromite and nickel arsenides associated with orthopyroxene, cordierite or both. The ores occur in veins or layers less than 70 cm in thickness and between 15 and 50 m long, which show sharp contacts with the host peridotites and are discordant to their foliation. These ores are generally found in the spinel tectonite and granular peridotite domains (Fig. 2) and form layers of massive chromite with nickel arsenides [mainly nickeline (NiAs) but also nickeliferous löllingite ($(Fe,Ni,Co)As_2$)] and minor ilmenite (in orthopyroxene-bearing ores) or rutile (in cordierite-bearing ores), alternating with (or grading laterally into) layers of pyroxenites or *cordieritites* (>90% cordierite). The size of chromite grains varies from 0.005 to 0.6 mm and their crystal habit is function of the modal proportion of Ni-arsenides. In ores rich in nickel arsenides (20–40% in volume) chromite grains tend to be euhedral to rounded or show dissolved grain boundaries within a nickeline matrix (>90% in volume). In ores poor in nickel arsenides (<10% in volume) chromite displays a polygonal pattern with nickeline blebs located in triple points. Chromite often hosts inclusions of orthopyroxene, phlogopite, wonesite, magnesian chlorite, quartz, nickeline, nickeliferous löllingite, parammelsbergite ($NiAs_2$), pyrite, pyrrhotite and chalcopyrite, as well as lamellae-like exsolutions of ilmenite or rutile. *Cr-Ni* ores are rich in gold (up to 35 ppm) and have nearly chondritic platinum-group element abundances (up to 1 ppm Pt + Pd; Gervilla and Leblanc, 1990; Leblanc et al., 1990). These noble metal contents are positively related to the proportion of Ni-arsenides in the rock. The role of Ni-arsenides as collector of the noble metals was demonstrated by *in situ* analysis using micro-PIXE by Gervilla et al. (2004) and more recently using LA-ICPMS by Piña et al. (2015), who measured up to average 25 ppm of Pd in maucherite and average 48 ppm of Pt in nickeliferous loellingite.

Interestingly, some ore occurrences in the Serranía de Ronda show mineralogical, textural and chemical evidence (e.g., compositional trends of chromite) transitional between the styles of mineralization described above, suggesting a possible common origin. Furthermore, the occurrence of each end-member ore within a given petrological-structural domain of the massifs links the genesis of these ores to magmatic processes (Gervilla and Leblanc, 1990; Gutiérrez-Narbona, 1999; Gutierrez-Narbona et al., 2003; González-Jiménez et al., 2013b).

3. Description of the samples

In this study, we focus on three Cr-Ni ore bodies in the Serranía de Ronda massifs (Fig. 2), namely the Ni-arsenide poor chromitite body from Arroyo de la Cala (Ronda massif) and the Ni-rich arsenide chromitite ± cordieritite bodies of Barranco de las Acedías (Ronda massif) and La Gallega Mine (Ojén massif). Previous work (Oen, 1973; Oen et al., 1973; Gervilla and Leblanc, 1990; Gervilla et al., 1996, 1999) provided the petrological and geochemical characterization of the Cr-Ni ores analysed in this study, including their bulk-rock major- and trace-element analyses. Therefore, here we only provide a brief description of the zircon-bearing ores considered in this study.

3.1. The Cr-Ni ore body of Arroyo de la Cala, Ronda massif

This mineralization consists of a Ni-arsenide poor (<1 vol% arsenides) chromitite body hosted in depleted dunite-harzburgite within plagioclase tectonites, close to the contact with the overlying granular peridotites (Fig. 2). The ore body is a sigmoidal lens (surface projection 9 × 5 m) made up of a stock-work of massive chromitite veins enclosing lenticular and layered bodies of orthopyroxenites and angular blocks of country rocks (Fig. 3a–c), including harzburgite, dunite and pyroxenite layers (Fig. 3a–d). The contacts with these blocks of country rocks are networks but there is a complete gradation from one massive chromitite to orthopyroxenite (Fig. 3b–d). In the latter case, orthopyroxene (the main silicate phase included in chromite) is optically continuous with the orthopyroxene of the neighboring orthopyroxenite. The massive chromitite shows vertical foliation and lineation parallel to the shear zones associated with development of the plagioclase tectonite domain, indicating high-temperature deformation of the unconsolidated ore, possibly related to syntectonic magmatic crystallization (Hidas et al., 2013). Zircons were recovered from one massive chromitite sample (sample 7R12-4; Fig. 3e, f).

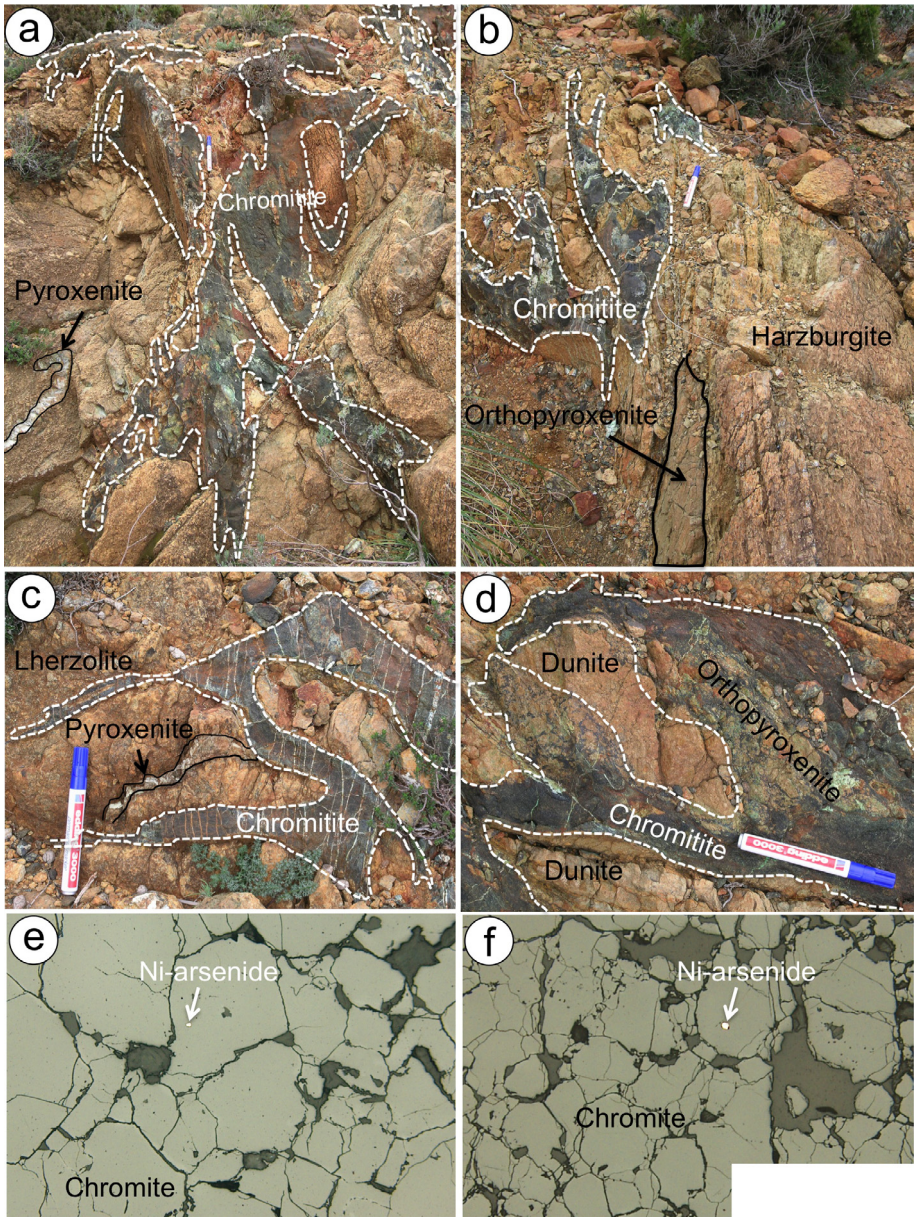

Fig. 3. Field photographs (a–d) and reflected light photomicrographs (e–d) of the Arroyo de la Cala Ni-arsenide poor chromitite ore (Ronda massif). (g) Field photograph of the Barranco de las Acedías (Cr-Ni)-cordieritite outcrop (Ronda massif). (h–j) Photograph of the (Cr-Ni)-cordieritite-plagioclasite of the La Gallega Mine (Ojén massif). (k, l) Reflected light microphotographs of the Ni-arsenide rich chromitite and orthopyroxenite of the La Gallega mine.

3.2. The Cr-Ni-cordierite ore of Barranco de las Acedias, Ronda massif

This ore crops out in the SW portion of the spinel tectonite domain of the Ronda massif, very close to the recrystallization front (Fig. 2). It is a small dyke (25 cm thick) of massive chromitite rich in Ni-arsenides (>10 vol%), intergrown with an orthopyroxenite that laterally grades to massive cordieritite (Fig. 3g). Zircons were only recovered from massive cordieritite (sample 9R12-1).

3.3. The (Cr-Ni)-cordierite ore of la Gallega Mine, Ojén massif

The abandoned mine of La Gallega is located in the southwesternmost part of the Ojén massif, near the town of Ojén (Fig. 2). The ore was exploited in the past century and consisted of several dyke-like bodies half a meter in thickness, which extended >100 m and are discordant to the foliation of the enclosing peridotite (Figs. 3h, i). Observations in the unexploited part of the mine indicate that the ores from a network of veins consisting of fine-grained mixtures of massive Ni-arsenides and chromite (Fig. 3k). These veins are hosted in orthopyroxenite that laterally grades to massive cordieritite, which also contains veins of chromite (Fig. 3h, i). Hernández-Pacheco (1967) described cordieritite veinlets unrelated to the Cr-Ni mineralization, but our field observations indicate that these rocks are always associated with Cr-Ni ores. Orthopyroxenite samples often contain chromite and interstitial Ni-arsenides (Fig. 3l), and chromite in the chromitites host large inclusions of orthopyroxene. The cordierite-rich samples are made up of large cordierite crystals with inclusions of chromite and Ni-arsenides, grading to polygonal textures made up of fine-grained aggregates of ore (Fig. 3k). The Cr-Ni veins and the associated pyroxenite-cordierite rocks are locally cut by leucocratic dykes (hereafter plagioclasites; Fig. 3j) made up of plagioclase, cordierite and phlogopite with accessory amounts of chromite, nickeline and zircon. In other Cr-Ni ores in the Ronda massif (e.g., Los Jarales;

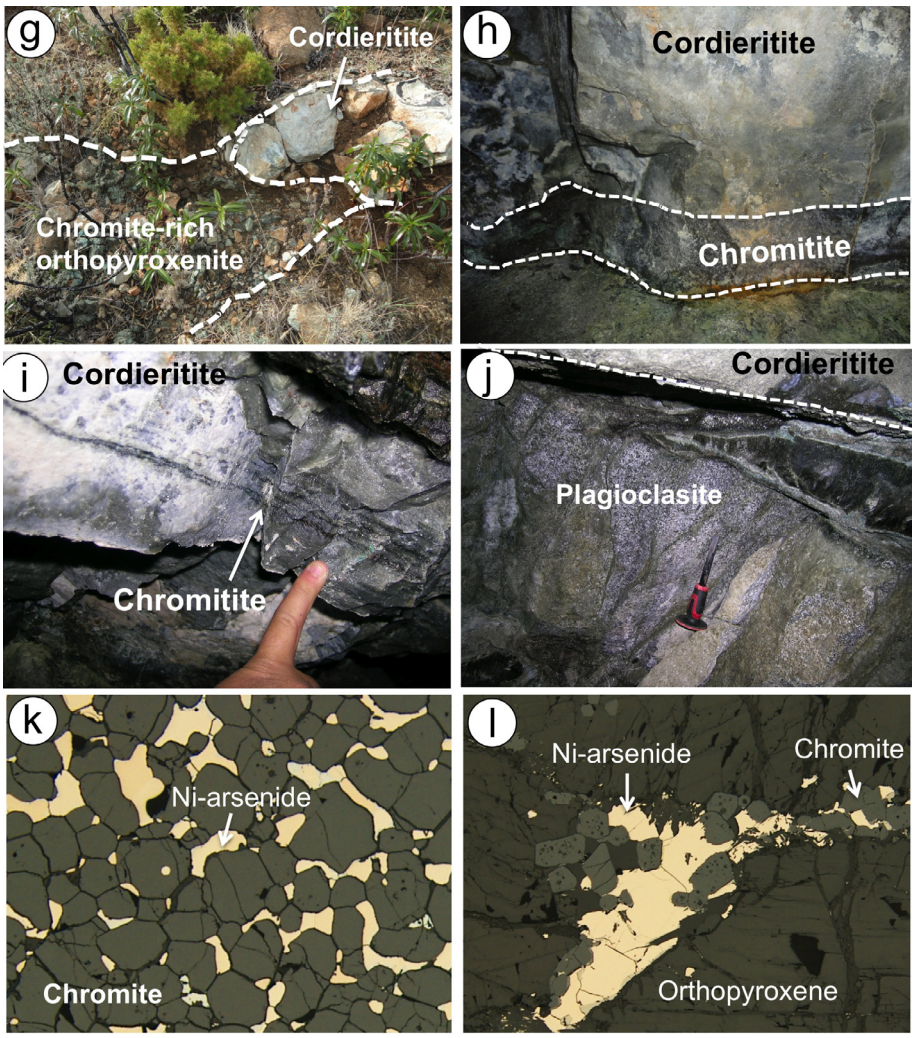

Fig. 3 (*continued*)

Gervilla, 1990), plagioclasites constitute the lateral extension of massive cordieritite but this relationship was not observed in the La Gallega mine. Zircons were recovered from three samples: (1) a massive chromitite (sample 1LG-1), (2) a plagioclasite dyke (sample 1LG-2), and (3) a massive cordieritite (sample 1LG-3).

4. Analytical procedures

Analytical procedures and results of *in situ* U-Pb, Lu-Hf and O isotopic analyses of zircons are described in detail in the available online Appendix 1, 2, 3 and 4.

5. Results

5.1. The Cr-Ni ore body of the Arroyo de la Cala, Ronda massif

Only six zircons were recovered from one sample of massive chromitite from this ore body (sample 7R12-4), five of which were analysed by ion microprobe (Fig. 4; Appendix 2, 3, and 4):

(1) Grain Zr-1 and Zr-6 are euhedral and their cathodoluminiscene (CL) images show continuous oscillatory zoning (Fig. 4). Zr-1 yields a discordant age at 2309 ± 37 Ma (1σ uncertainty) and has a relatively low U content (339 ppm) and $\delta^{18}O = 5.5‰$, whilst Zr-6 provides a concordant age at 1804 ± 5 Ma (1σ uncertainty) and has much higher U content (1239 ppm) and higher $\delta^{18}O = 8.3‰$ (Fig. 4; Appendix 2, 3 and 4).

(2) Grains Zr-3 and Zr-4 are round in shape and their CL images show partly resorbed cores overgrown by a broad oscillatory-zoned rim with either higher or lower CL emission (Fig. 4). Four SIMS analyses of the cores and rims of these zircons yield condordant ages (Appendix 2 and 4). The ages of the core and the rim of grain Zr-4 matches within error (core: 1815 ± 9 Ma, rim: 1794 ± 17 Ma) whilst the core of grain Zr-3 is older (192 ± 13 Ma) than its rim (109 ± 15 Ma) (Fig. 4; Appendix 2 and 4). Reliable oxygen-isotope data ($\delta^{18}O = 9.4‰$) were only obtained for the core of zircon grain Zr-3 (Fig. 4; Appendix 3).

(3) Grain Zr-2 is a broken crystal with a barely visible oscillatory zoning (Fig. 4). The SIMS analysis of this zircon yields a concordant age at 1207 ± 34 Ma (Fig. 4; Appendix 2 and 4).

5.2. The Cr-Ni-cordieritite of Barranco de las Acedías, Ronda massif

Eleven zircon grains recovered from the cordieritite sample 9R12-1 are rounded grains and larger than 50 μm. The CL images show composite zircons with partly resorbed cores overgrown by structureless rims (Fig. 5). Nine zircons were analysed by LA-MC-ICPMS and six of them yield scattered concordant ages between

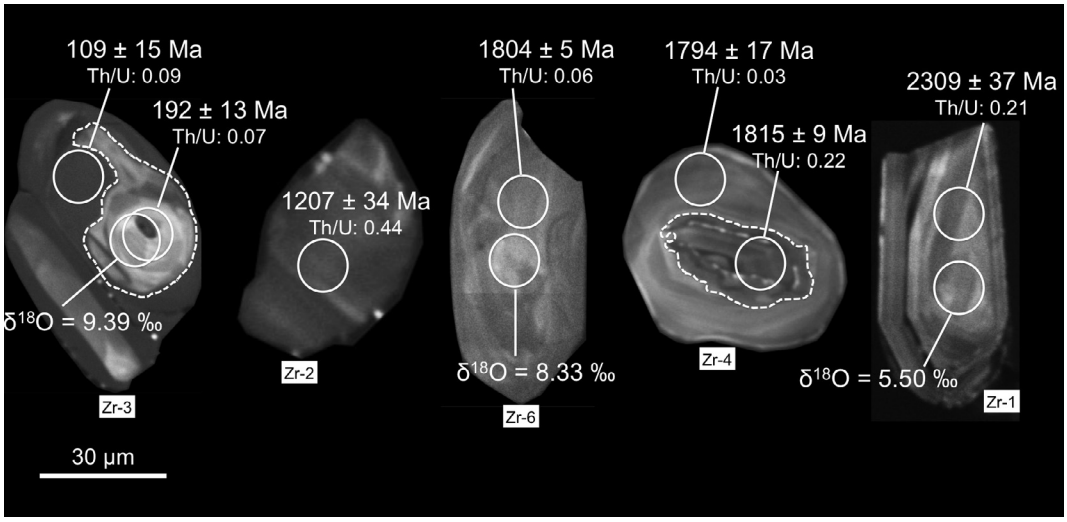

Fig. 4. Cathodoluminiscene (CL) images of zircon grains from the massive chromitite of the Arroyo de la Cala Cr-Ni ore (Ronda massif; sample 7R12-4).

576 ± 11 Ma and 21.2 ± 0.4 Ma (the latter age obtained from the rim of Zr-3 in Fig. 5; Appendix 2 and 4). Most of these zircons (whether with concordant or discordant ages) have high $\delta^{18}O$ (7.1–13.5‰) and unradiogenic Hf-isotope ratios ($\varepsilon_{Hf}(t)$ from −12.36 to −6.7; Appendix 3). In contrast, three zircons (Zr-2, Zr-4 and Zr-8; Fig 5) that yield concordant Cambrian to Neoproterozoic ages (536.9 ± 9.5 Ma to 568 ± 10 Ma) exhibit decoupled O- and Hf-isotope signatures, characterized by $\delta^{18}O$ (4.8–5.9‰) overlapping the typical mantle range (5.3‰ ± 0.6‰; Valley et al., 1998, 2005; Valley, 2003), but $\varepsilon_{Hf}(t)$ (−5.81 to −4.43) lower than normal mantle values (Appendix 3).

5.3. The Cr-Ni-cordieritite of la Gallega Mine, Ojén massif

Four zircons were separated from a massive chromitite (sample 1LG1), which are euhedral-elongated grains with either oscillatory or sector zoning parallel to crystal faces (Fig. 6). In the CL imaging, these grains show continuous oscillatory zoning (Fig. 6). The SIMS data of these four grains yield concordant or nearly concordant ages ranging from 19.8 to 21.0 Ma and provide a mean $^{206}Pb/^{238}U$ age of 20.4 ± 0.87 (MSWD = 2.4 and probability = 0.063; Appendix 4). The LA-MC-ICP-MS analyses yield unradiogenic Hf-isotope values corresponding to $\varepsilon_{Hf}(t)$ between −7.3 and −12.1 (Appendix 3).

Twenty-one zircons recovered from another massive cordieritite (sample 1LG3) were dated using LA-ICP-MS (Fig. 7 and Appendix 2). Many of them are rounded grains with complex internal CL structures characterized by cloudy high-luminescence patterns, although a few grains exhibit continuous oscillatory zoning (Fig. 7). These zircons yield scattered concordant, subconcordant and discordant U-Pb ages varying from 33.8 ± 1 Ma to 781 ± 10 Ma as well as variable U-contents (105–13,865 ppm) and Th/U ratios (0.003–0.8). Three different populations can be distinguished on the basis of O- and Hf-isotope compositions, which are unrelated to age. The first population includes most of the analysed grains (ages from 33.8 ± 1 Ma to 781 ± 10 Ma) and it is characterized by consistently high $\delta^{18}O$ (6.01–12.7‰) and negative $\varepsilon_{Hf}(t)$ (from −14.42 to −6.88). The second population includes three grains that yield discordant ages of 119.1 ± 0.9 Ma, 189 ± 2 Ma and 376 ± 3 Ma and exhibit high $\delta^{18}O$ (7.6–11.1‰) but positive $\varepsilon_{Hf}(t)$ (3.10–4.84). The third population consists of two grains (only one dated, with discordant age of 212 ± 1 Ma) with $\delta^{18}O$ <5.5‰.

Several zircons were recovered from a plagioclasite dyke (sample 1LG2). In the CL imaging, all these crystals show continuous oscillatory zoning parallel to the outer shape of the grain (Fig. 8). The LA-ICP-MS data obtained from eleven of these zircons yield high average U-contents (3685 ppm) and average Th/U ratios (0.11) (Fig. 8 and Appendix 2), and ages scattering between 20.1 ± 0.2 Ma and 17.9 ± 0.1 Ma (Fig. 8 and Appendix 2), with a weighted mean $^{206}Pb/^{238}U$ age of 18.5 ± 0.3 (MSWD = 22, 1σ uncertainty Appendix 3). These zircons are characterized by heavy oxygen isotopes ($\delta^{18}O$ = 11.3–12.4‰) and unradiogenic Hf-isotopes ($\varepsilon_{Hf}(t)$ between −14.5 and −7.6).

6. Discussion

6.1. Crustal zircon xenocrysts recycled in the Arroyo de la Cala Ni-arsenide poor chromitite

The ages of 1815 ± 9 Ma to 1794 ± 17 Ma exhibited by the core and rim of zircons grain Zr-4 from the Arroyo de la Cala chromitite (Fig. 4) match well with the U-Pb age (1783 ± 37 Ma) of the inherited core of a zircon in garnet pyroxenite from the spinel tectonite domain of Ronda (Sánchez-Rodriguez and Gebauer, 2000). Likewise, the SIMS analysis of the core of the zircon grain Zr-3 extracted from this chromite ore (Fig. 4) yields a concordant Early Jurassic age (192 ± 13 Ma; Appendix 2) which is consistent, within error, with the ages of 180 ± 5 Ma and 178 ± 6 Ma reported for magmatic zircons in the garnet pyroxenite containing the Proterozoic zircon core mentioned above (Sánchez-Rodríguez et al., 1996; Sánchez-Rodriguez and Gebauer, 2000). Similarly, the concordant age of 109 ± 15 Ma recorded in the rim of our zircon grain Zr-3 (Fig. 4 and Appendix 2) is close to the concordant age (131 ± 3 Ma) of a population of zircons in a corundum-bearing garnet pyroxenite from the Ronda massif (Sánchez-Rodriguez and Gebauer, 2000). Field evidence indicates that the Arroyo de la Cala Cr-Ni ore is intimately associated with Cr-rich orthopyroxenites (type D of Garrido and Bodinier, 1999), which formed by reaction of pre-existing garnet pyroxenite with basaltic melts of boninitic affinity in the Late Oligocene-Early Miocene (Gervilla and Leblanc, 1990; Gutierrez-Narbona, 1999; Garrido and Bodinier, 1999; Marchesi et al., 2012). Therefore, zircons of the Arroyo de la Cala Cr-Ni ore are interpreted as xenocrysts recycled from precursor garnet pyroxenites.

Zircon-bearing garnet pyroxenites of Ronda display strong geochemical evidence of being related to oceanic/arc crust (Sánchez-

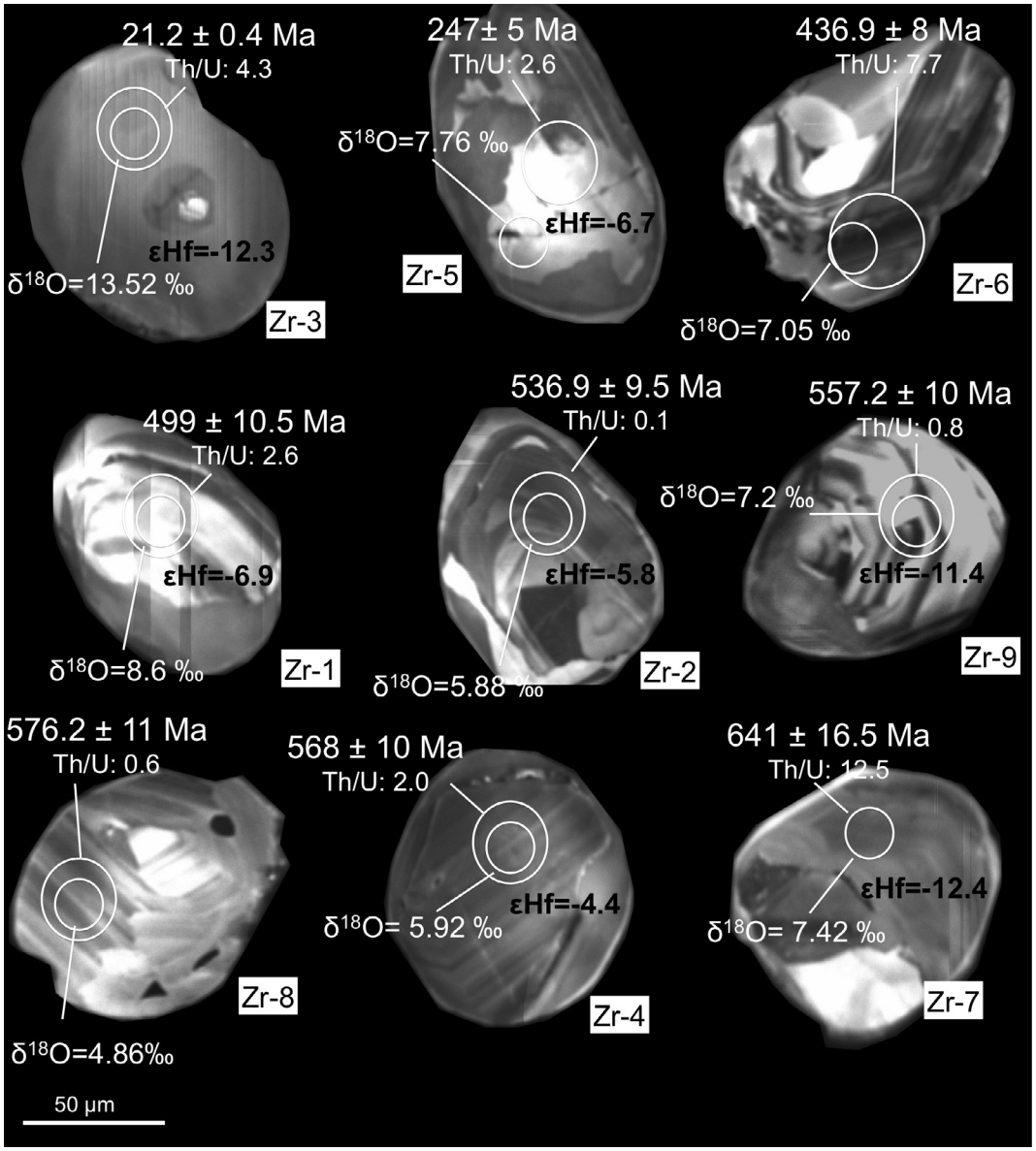

Fig. 5. CL images of zircon grains from the massive cordieritite of Barranco de las Acedías (Ronda massif; sample 9R12-1).

Rodríguez et al., 1996; Sánchez-Rodriguez and Gebauer, 2000; Downes, 2007), very likely to cumulate gabbros, which were recycled at very high pressures (>1.5 GPa) in the mantle (Garrido and Bodinier, 1999; Morishita et al., 2001, 2003, 2009; Marchesi et al., 2013). Indeed, the age of 109 ± 15 Ma recorded in the rim of our Early Jurassic zircon provides a minimum age of this crust. If so, Mesozoic zircons could be magmatic crystals from: (1) the gabbroic part of the oceanic/arc crust subducted/delaminated/det ached and foundered in the mantle (2) (meta)sediments associated with this crust, or (3) disrupted pieces of continental crust tectonically mixed with the oceanic/arc crust during subduction in the Late Oligocene-Early Miocene. However, we cannot discriminate between these three possible origins on the basis of the available data.

The other Proterozoic zircons of ~1800 Ma identified in the Arroyo de la Cala Cr-Ni ore and in the garnet pyroxenites documented by Sánchez-Rodriguez and Gebauer (2000) are also inherited grains. The relatively high $\delta^{18}O$ (8.3‰) exhibited by one of these zircons (i.e., grain Zr-6 in Fig. 4 and Appendix 2 and 3) argues for a crustal origin, although possible alteration by crustal-derived fluids cannot be ruled out owing to its discordant age (Appendix 4). Interestingly, the peridotites of the Ronda and Ojén massifs preserve a common population of base-metal sulfides that yields rhenium-depletion T_{RD} model ages of 1.6–1.8 Ga. These model ages have been interpreted as the time when these ultramafic massifs were isolated from the convecting mantle and were incorporated into the subcontinental lithosphere (Marchesi et al., 2010; González-Jiménez et al., 2013a,b). Our data thus support the idea that the inherited Proterozoic zircons may be relicts of the ancient continental crust produced during this event.

From our observations above, it is clear that crustal zircons in the Arroyo de la Cala Cr-Ni ores suffered an almost complete pathway of recycling. They crystallized at low-pressures from a melt in the oceanic or continental crust, then they were buried to relatively great mantle depths (marked by the formation of garnet pyroxenites) and carried to shallow mantle domains by migrating basaltic melts during exhumation. Indeed, successive cycles of partial melting and crystallization of pyroxenites in the upper mantle constitute an effective mechanism for transporting xenocryst zircons through different segments of the lithosphere in subduction

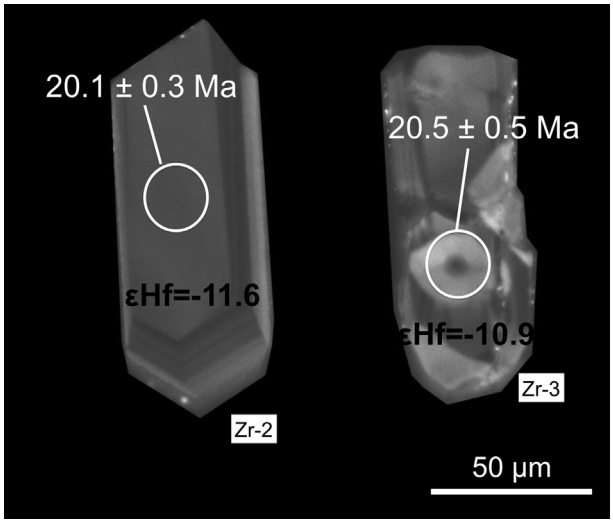

Fig. 6. CL images of zircon grains from the massive chromitite of the La Gallega mine (Ojén massif; sample 1LG-1).

zones. However, how did these crustal zircons survive under high P-T conditions in the Earth's mantle while their U-Pb isotopic compositions remained unchanged?

The pressure and temperature of equilibration estimated for pre-kinematic, coarse-grained garnet lherzolite assemblages in Ronda are 2.4–2.7 GPa and 1020–1100 °C (Garrido et al., 2011). These estimates allow us to define an upper pressure limit for the recycling of crustal material in Ronda under conditions where $ZrSiO_4$ is still stable [synthetic $ZrSiO_4$ transforms to the high-P polymorph reidite at 12–15 GPa and 900 °C (Reid and Ringwood, 1969; Liu, 1979) or at 8–10 GPa and 900–1400 °C (Ono et al., 2003)]. Therefore, high pressure conditions leading to polymorphic transformation and change of the zircon U/Pb compositions can be ruled out. Furthermore, Morishita et al. (2001) demonstrated that the Ronda's zircon-bearing corundum-garnet pyroxenites formed at *ca* 1–1.5 GPa and 800–900 °C. These P-T conditions are favourable for preserving the Pb isotope compositions in recycled zircons.

Little or no interaction with the parental melts of the Cr-Ni ores may explain the preservation of idiomorphic zircons with meanigful geological ages (e.g., Zr1 and Zr 6; Fig. 4 and Appendix 4). For example, the equilibration of zircons with surrounding melt may have been inhibited by their rapid transfer by porous flow in small melt pockets from the garnet pyroxenites source to a new site in chromite (Bea et al., 2001), or their inclusion in shielding minerals like pyroxene, olivine or chromite (e.g., Gebauer, 1996; Zhou et al., 2014). Both scenarios are compatible with each other and are consistent with the following observations: (1) the Arroyo de la Cala chromitite is very close to the Ronda re-crystallization front, which indicates a short distance of migration of the parental melts from their source (i.e., the granular peridotite domain); (2) low melt/rock ratios during migration of the small volume melts parental of the chromitite that would allow porous flow through small pore reservoirs (Lenoir et al., 2001; Marchesi et al., 2010; González-Jiménez et al., 2013b and references therein); and (3) the Cr-Ni ores crystallized from small volumes of melts that underwent a very rapid undercooling (from ~1200 to 800 °C), associated with the final ascent of the host peridotites (at upwelling rates of 0.4 cm/year from 800 to 900 °C and decompression from 0.7 to 0.5 GPa; Obata, 1980; Platt et al., 1998; Hidas et al., 2013). This process induced rapid crystallization of early magmatic phases, such as olivine, chromite and pyroxenes, which trapped the xenocryst zircons and likely protected them from the surrounding melt.

6.2. Co-magmatic and inherited zircons in the chromitite-cordierite ores

The age of 20.4 ± 0.87 Ma obtained for the four zircons from the Ni-arsenide rich chromitite of La Gallega Mine (Ojén massif) is indistinguishable, within error, from the age of 18.5 ± 0.3 Ma of zircons in its neighboring plagioclasite. Moreover, this age coincides with that of the structureless zircon rim from the cordieritite of Barranco de las Acedias in the Ronda massif (21.2 ± 0.4 Ma). Leucogranites crosscutting the peridotites in the Ronda massif contain zircons of similar ages [18.9 ± 3.0 Ma (Sánchez-Rodriguez and Gebauer, 2000) and 21.8 ± 0.5 Ma (Esteban et al., 2007)] as well as similar oscillatory or sector zoning parallel to well-developed external faces (Fig. 8; Sánchez-Rodriguez and Gebauer, 2000; Esteban et al., 2007, 2011), suggesting that the crystallization of all these zircons occurred in a melt. Moreover, zircons from the chromitite and plagioclasite have elevated $\delta^{18}O$ values (11.1–12.3‰; Fig. 8) that overlap the bulk-rock composition of the leucogranite dykes in Ronda, suggesting a possible common source. The highly negative $\varepsilon_{Hf}(t)$ values of zircons from chromitite (−12.1 to −7.3) and plagioclasite (−14.5 to −7.6) suggest a crustal source, consistent with the interpretation of the leucogranitic dykes in Ronda as anatectic melts of country metasedimentary rocks produced during the emplacement of the hot peridotites into the middle crust (Priem et al., 1979; Acosta, 1997). The introduction of these crustal zircons into the already-formed chromitites by late fluids can be ruled out on the basis of the mutual intergrowth of cordieritite and chromitite and the gradual transitions of the cordieritite to the plagioclasite, which are indicative of crystallization from a common evolving melt (see below).

A great number of zircons recovered from the massive cordieritite samples show variable $\delta^{18}O > 6–7.5‰$ and correspondingly negative $\varepsilon_{Hf}(t)$ (−14.4 to −6.7), typical of crustal zircons. The ages of these zircons scatter from 33.8 ± 0.7 Ma to 781 ± 5 Ma, and their Th/U ratio varies from typically magmatic (>0.2) to metamorphic values (~0.01). Most of these zircons show round, possibly corroded edges and cloudy complex zoning patterns in CL images (Figs. 5 and 7), similar to zircons documented in anatectic rocks of the footwall of the Ronda peridotite, specially those from the metapelites of the Jubrique unit (Acosta-Vigil et al., 2014 and references therein). These zircons clearly support the crustal origin of the cordieritites, which could form in the early stage of fractionation of highly peraluminous granitic melts and migmatites, or be migmatites themselves formed by melting of the country metasediments (Rapela et al., 2002; Giuliani et al., 2007; Thiéry, 2011). Interestingly, the crosscutting cordierite-bearing leucogranite dykes in the Ronda and Ojén ultramafic bodies probably crystallized from highly peraluminous granitic melts produced by melting of metasediments (Tubía, 1985; Tubía and Cuevas, 1986; Tubía et al., 1997; Acosta et al., 1997; Pereira et al., 2003; Cuevas et al., 2006). As noted above, these dykes intruded the peridotites almost contemporaneously with the cordieritites and plagioclasites studied here.

Indeed, the lateral gradation of cordieritites to leucogranites and plagioclasites might indicate derivation from a common parental melt. Thus, an early segregation of cordieritites could have depleted a precursor anatectic highly-peraluminous granitic melt in mafic components, producing a more evolved felsic segregate that eventually crystallized leucogranites (e.g., Rapela et al., 2002), plagioclasites (Gervilla, 1990) and liberated volatile-rich siliceous fluids. Late felsic fluids are rich in Si, Al, Na, K, Ca and Cl as well as in fluid mobile elements such as LILE, Sr and Pb, but they are poor in Mg and Fe (Pereira et al., 2003; Esteban et al., 2011), like the fluids released during dehydration of metasediments in subducting slabs (Yaxley and Green, 1998; Proteau et al., 2001; Manning, 2004; Berly et al., 2006; Grant et al., 2016). The reaction

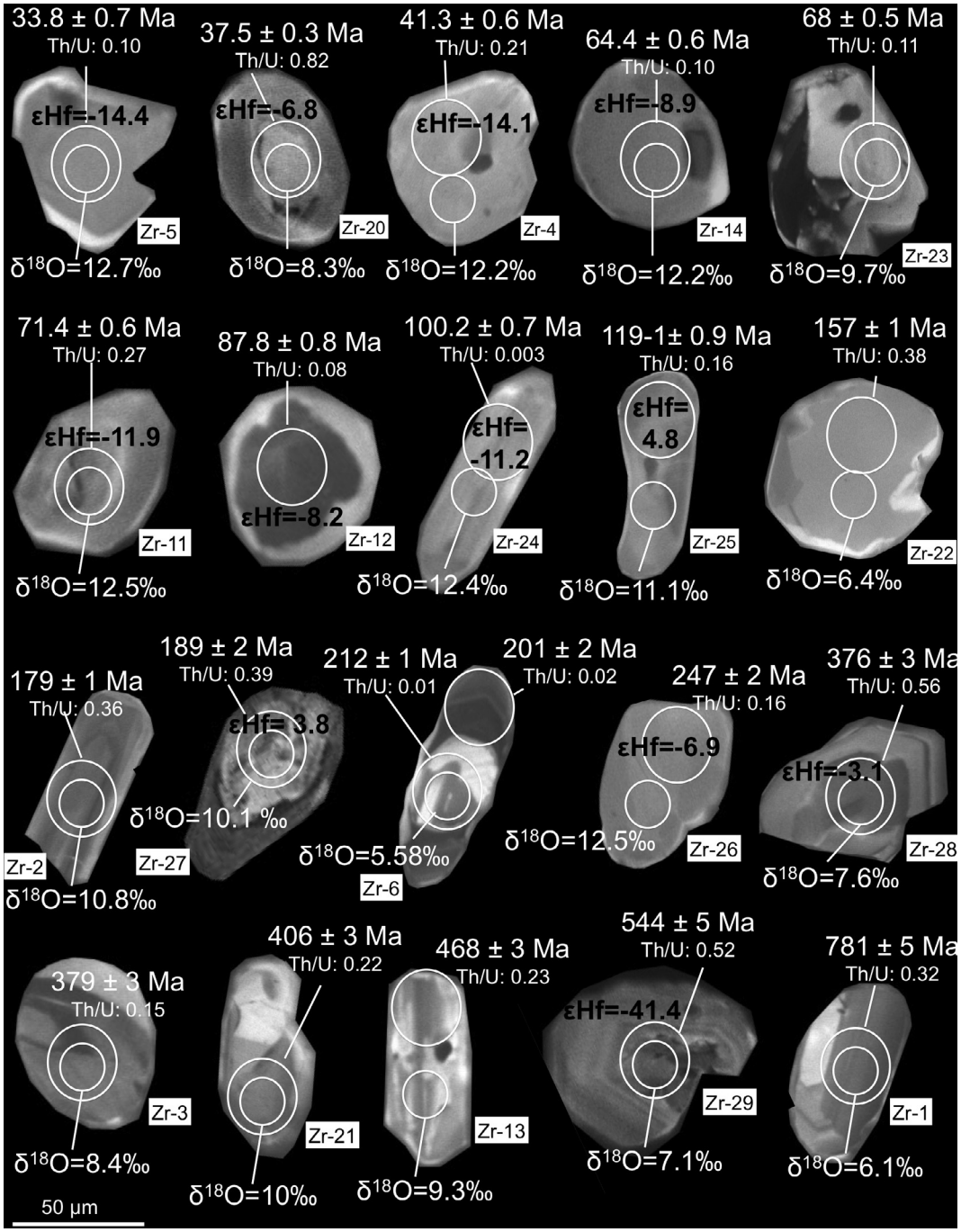

Fig. 7. CL images of zircon grains from the massive cordieritite of the La Gallega mine (Ojén massif; sample 1LG-3).

of this siliceous fluid-rich phase with an already fractionated mantle-derived (ultra)mafic melt (see next section), which was enriched in metals (PGE and Au), As and other volatile components (S, C, Cl, and F), likely produced a hybrid "exotic" pyroxenitic melt from which the Cr-Ni ores crystallized (Oen 1973; Oen et al., 1973; Gervilla and Leblanc, 1990). Chromite could precipitate from the hybrid melt produced during mixing, as the solubility of Cr in mafic melts drops when silica is added (Irvine, 1975; Bédard and Hérbert, 1998; Ballhaus, 1998; Edwards et al., 2000). In this scenario, the Aquitanian (~20 Ma) zircons found in chromitites may have grown metasomatically in the mantle, but inheriting a crustal-like signature similar to that of the contemporaneous zircons of the cordieritite and plagioclasite. Our observations can elegantly explain the crustal signature observed in zircons grown in the mantle from fluids or melts fluxed from deeply subducted crust into overlying mantle wedges (Liati and Gebauer, 2009; Liu et al., 2010; Li et al., 2016).

In this model, the scarcity of Aquitanian zircons in the cordieritites and associated chromitites might reflect the very rapid crystallization of the early-segregated cordieritic melt, which would have inhibited the crystallization of co-magmatic zircons. This cordieritic melt was probably undersaturated in Zr, as lithophile elements were preferentially concentrated in the residual leucocratic melt from which the plagioclasite crystallized. The intrusion of this anatectic melt is bracketed between 21.2 ± 0.4 Ma and 18.54 ± 0.3 Ma, corresponding to the ages obtained

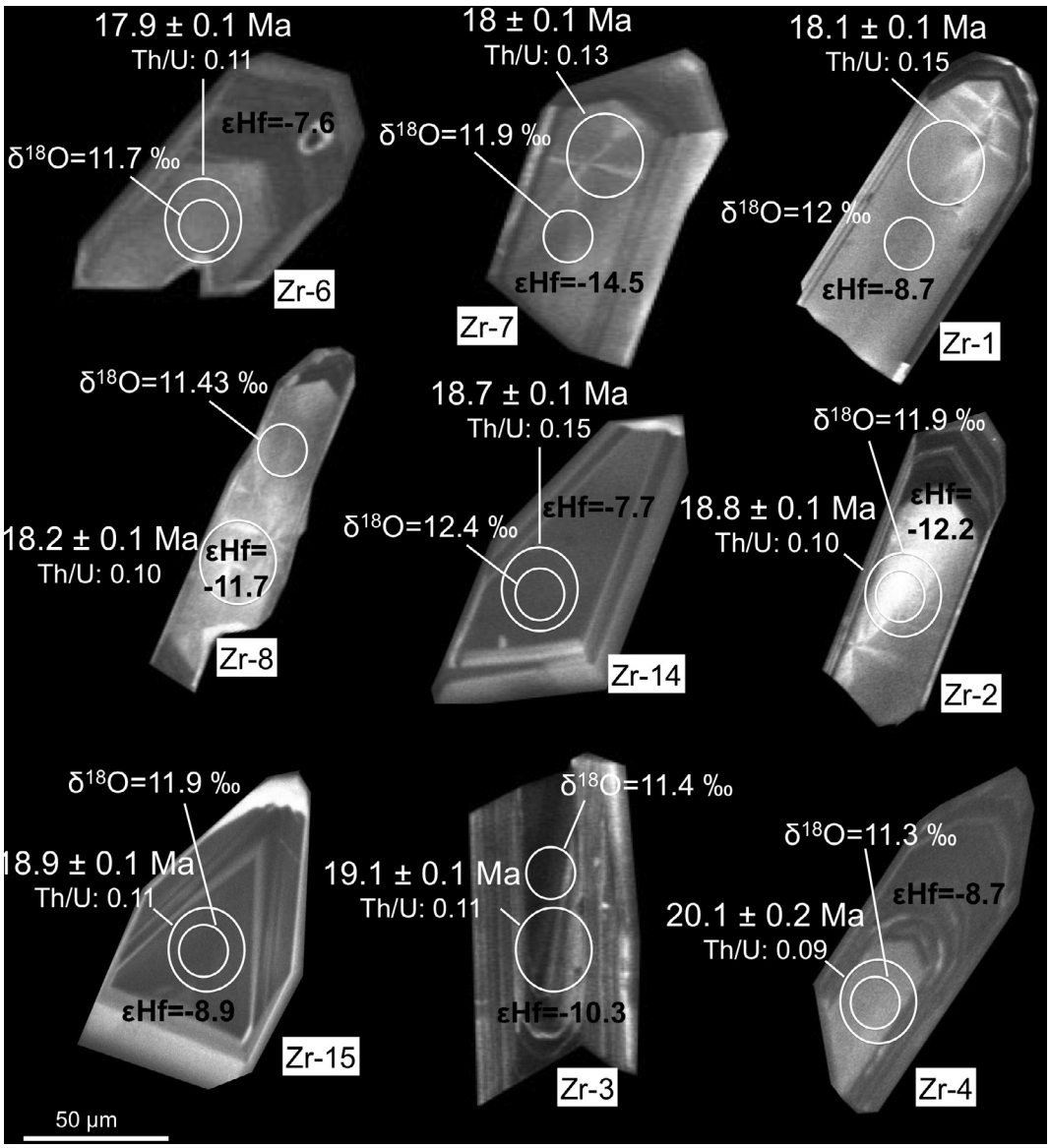

Fig. 8. CL images of zircon grains from the plagioclasite dyke of the La Gallega mine (Ojén massif; sample 1LG-2).

for the structureless zircon rim from the cordieritite of Barranco de las Acedias (Ronda massif), and that obtained for zircons of the plagioclasite from the La Gallega mine (Ojén massif).

6.3. Genesis of the Cr-Ni ores during crustal underthrusting and coeval emplacement of the peridotites

The geology and tectonic evolution of the western Mediterranean indicate that during the Late Oligocene-Early Miocene, the SCLM represented by the Ronda peridotites was located at the rear of a continental arc (i.e., the Alboran wedge; Garrido et al., 2011) that consumed the Tethys oceanic lithosphere in the central areas of the arc and collided laterally with the Maghrebian and South Iberian paleomargins in the Early to Late Miocene (Fig. 9; e.g., Hidas et al., 2013 and references therein). Garrido et al. (2011) suggested that southward to westward retreat of the slab during the Late Oligocene-Early Miocene enhanced intense back-arc lithosphere extension (Faccenna et al., 2004; Booth-Rea et al., 2007) and the development of an extensional shear zone in the Ronda peridotite, coeval with extreme thinning of the Alboran overlying crust. Hidas et al. (2013) showed that inversion of this back-arc basin in the Late Oligocene-Early Miocene resulted in km-scale folding and shearing of the attenuated SCLM (Fig. 9a). These events led to underthrusting of the continental crust beneath the peridotites, and eventually to the intracrustal emplacement of the massif into the Alboran wedge and its final thrusting at 17 Ma (Esteban et al., 2011).

During the earliest stages of thinning of the SCLM in the Late Oligocene-Early Miocene (~25 Ma), large volumes of melts from the upwelling asthenosphere migrated upward and infiltrated the thinned lithospheric mantle while promoting its pervasive melting (Van der Wal and Bodinier, 1996; Garrido and Bodinier, 1999; Lenoir et al., 2001; Marchesi et al., 2012). The rapid ascent of the peridotites (upwelling rates of 0.4 cm/year; Platt et al., 1998) very likely caused the cooling of the shallowest mantle and prevented the upward progression of the partial-melting and melt-migration front, i.e., the recrystallization front of Van der Wall and Vissers (1993). Upward-migrating melts reacted with the host peridotite to form clinopyroxene and segregated small fractions of volatile-rich melts (Lenoir et al., 2001). These small-volume melts

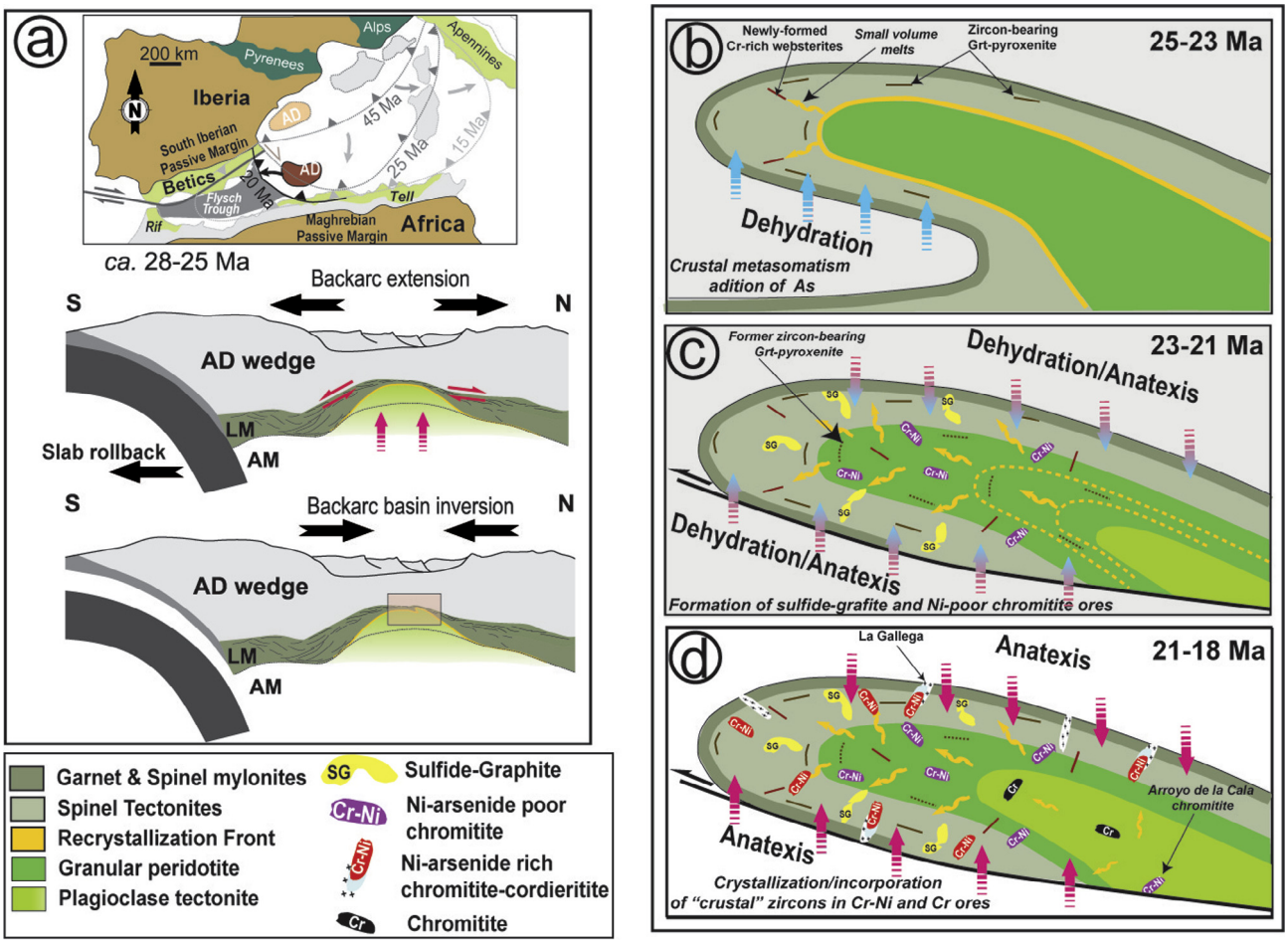

Fig. 9. Sketches showing the tectonic evolution of the Western Mediterranean realm in the Cenozoic (a–c) and the genesis of the different ores within the mantle peridotites during the development of a fold-thrust structure (b–d). Modified from Hidas et al. (2013). Legend inset in the figure.

were channelled above the recrystallization front through refractory peridotites. They were partially fractionated by the crystallization of interstitial clinopyroxene, or they were trapped into open fractures forming intrusive, Cr- and Mg-rich pyroxenite dykes (Garrido and Bodinier, 1999; Marchesi et al., 2012). This event took place coevally with the initiation of back-arc inversion (Hidas et al., 2013), which promoted the incorporation of the enclosing crustal units into the fold-thrust structure (Fig. 9b). In this scenario, the emplacement of hot peridotites promoted dehydration and later anatexis of the enclosing crustal units, especially of high-grade mylonitic gneisses (Fig. 9b–d; Acosta, 1997; Pereira et al., 2003; Cuevas et al., 2006; Esteban et al., 2007, 2011; Varas-Reus et al., 2016).

The infiltration of fluids derived from dehydration of the metasediments likely produced metasomatism in the SCLM, thus explaining the relatively high arsenic contents of peridotites and the light (biogenic) carbon signatures of the sulfide-graphite (S-G) ores (Crespo et al., 2006) (Fig. 9c). The first melts that reached the recrystallization front were likely generated by partial melting (and melt-rock reactions) of relatively fertile peridotites and pyroxenites pre-enriched in Ni-arsenides (Lorand, 1983) and graphite (also in graphitized diamonds; Pearson et al., 1989; Davies et al., 1993; Crespo et al., 2006). As a result the first small-volume melt fractions that migrated upward to the recrystallization front were rich in Si, Al, Ti, and Fe, and concentrated volatile components (C, H_2O, F and Cl) as well as S, As and chalcophile elements (including noble metals). We conclude that these basaltic melts with a boninitic parentage (Marchesi et al., 2012) constituted the parental melts of the arsenide- and sulfide-rich S-G and Cr-Ni ores (Fig. 9c, d).

Progressive penetration of the hot peridotite slice into the crust locally caused crustal anatexis, producing highly-peraluminous melts that intruded the peridotites at *ca* 21–18 Ma ago (Fig. 9d). The injection of these melts into the peridotites took place through weak zones developed parallel to axial folding, which were also used by small fractions of highly fractionated mafic-ultramafic melts squeezed outwards from the advancing recrystallization front. The interplay of the felsic fluid-rich phase accompanying the formation of the anatectic melts, with incoming highly-fractionated mafic-ultramafic melts produced "exotic" mafic melts with exceptionally high contents of Cr, V, Ti, Fe, Ni, Co, Cu, Zn, Al and As, crystallizing the cordierite-(Cr-Ni) ores found above the recrystallization front in the spinel tectonite domain (Fig. 9d). Interestingly, the Cr-Ni ores found below the recrystallization front (e.g., at El Nebral) do not contain cordierite, indicating that the ingress of the acidic melt was restricted to the uppermost part of the ultramafic bodies. In this context, it is also probable that continuous folding of the peridotites during uplift and cooling promoted the crystallization of interstitial melts below the recrystallization front. Under these conditions, the amount of small-volume melts that crossed the front was progressively smaller. In addition, these small-volume melts were generated by partial melting (and melt/rock reactions) of more depleted peridotites, and as a consequence, they were relatively impoverished in Al, Ti,

V, Fe, As and S and chalcophile elements, and contained higher amounts of Cr and Mg. This can explain the mineralogical and chemical features of Cr-Ni ores located close to or below the recrystallization front (e.g., at El Lentisco and El Nebral; Fig. 2 and Fig. 9d), which consist of chromite with minor nickel arsenides (<10 vol%) associated with Mg-rich orthopyroxenites (Gervilla and Leblanc, 1990).

Further uplift and cooling of the ultramafic body displaced the front downwards towards the central part of the fold-thrust structure, restricting melt percolation to dunitic channels while forming layered granular peridotites (Van der Val and Bodinier, 1996) and a new generation of Cr- and Mg-rich pyroxenites (Fig. 9c, d). The parental melts of the latter pyroxenites had a boninite-like signature but a weaker imprint of crustal contamination (Garrido and Bodinier, 1999; Lambart et al., 2009; Marchesi et al., 2012). Thus, the Cr-Ni ores crystallized from these later melts were more depleted in Ni-arsenides (Arroyo de la Cala and the northern vein of Mina Baeza; Gevilla and Leblanc, 1990). The generation of both pyroxenites and Cr-Ni ores from a common subduction-related parental melt is suggested by the transitional contacts between pyroxenites and chromitites in the Arroyo de la Cala Cr-Ni ore (Fig. 3b), and the Cr-rich composition of the chromite typical of chromite crystallized from arc-type melts of boninitic affinity (Gervilla et al., 1999). These Cr- and Mg-rich melts parental of the chromitite derived from the reaction between migrating melts and former garnet pyroxenites, as indicated by the presence of identical populations of zircon in the Cr-Ni ores and the garnet pyroxenites (Fig. 9b–d). The percolation/injection of primitive basaltic melts and Si-rich melts (or melts from eclogites/pyroxenites), and the reaction of these infiltrating melts with garnet pyroxenites are also a suitable mechanisms to produce chromite ores in the upper mantle (Ballhaus, 1998; Gonzalez-Jimenez et al., 2014).

On the other hand, the observation that the Arroyo de la Cala Cr-Ni ore exhibits deformation before final consolidation (Gervilla and Leblanc, 1990) indicates that the injection of its parental melt through the shear zone was synchronous with the development of the plagioclase tectonites (Fig. 9d). This constrains the formation of the ore to the very latest stages of emplacement of the peridotite bodies into the crust. According to our geochronological constraints, this event occurred coevally or soon after the formation of the cordierite-(Cr-Ni) ores and the intrusion of the youngest undeformed leucocratic dykes ~18–19 Ma ago.

7. Conclusions

The Cr-Ni ores in the ultramafic massifs of the Serranía de Ronda contain distinctive zircon populations. Zircons in massive chromitite from the Arroyo de la Cala have Mesozoic and older ages, but their crustal signatures that were inherited from an ancient oceanic/arc crust recycled in the mantle. In contrast, zircons in the chromitite of the La Gallega Mine date the formation of the mineralization associated with the emplacement of the ultramafic rocks into the continental crust in the Early Miocene. The O and Hf isotope signatures of these zircons are identical to those of contemporaneous zircons recovered from the associated plagioclasite dyke, which is in turn similar to the signatures of widespread anatectic leucogranitic dykes crosscutting the Ronda and Ojén massifs. Zircons from cordieritites associated with chromitites or chromitite-bearing orthopyroxenites yield scattered concordant and discordant ages similar to zircons from the crustal rocks that enclose the ultramafic bodies. These zircons also show significant variations in $\delta^{18}O$ and $\varepsilon_{Hf}(t)$ typical of crustal sources. We conclude that melts and fluids derived from both mantle and crustal sources mixed in the SCLM during crustal underthrusting and generated the distinctive chromite ores of the Serranía de Ronda peridotite massifs. During the emplacement of the hot peridotites fluids and melts were released from the enclosing metasediments as a result of dehydration and anatexis. These fluids and melts infiltrated the peridotite carrying xenocrystic zircons from the metasediments and adding components that allowed the precipitation of new (i.e., metasomatic) zircons. Contemporaneously with this process, xenocristic zircons recycled back into the mantle by previous subduction events were released from host pyroxenites and transferred to the newly formed chromite ores. All these observations provide new evidence that the genesis of chromitites and other related ores in the ultramafic rocks of the Serranía de Ronda was associated with the emplacement of these SCLM sections into the continental crust.

Acknowledgements

Franco Pirajno, Editor-in-Chief Franco of Ore Geology Reviews, and Sisir K. Mondal, guest Editor of this volume "Chromite: Petrogenetic Indicator to Ore Deposits", are thanked for the final editing of this paper. E.B. Watson, M Whitehouse and one anonymous referee are also thanked for their constructive reviews of the paper. Basic funding for this research was supported by a FONDECYT Initiation Grant #11140005 to J.M. González-Jiménez entitled "*Decoding precious metals (platinum-group elements and gold) in upper mantle rocks of the Chilean Cordillera*", and by the MSI "*Millenium Nucleus for Metal Tracing along Subduction*" (NC130065). Support for fieldwork and sampling was provided by the Project CGL2014-55949-R "*Sistemas magmático-hidrotermales no convencionales: una fuente de metales escasos*" funded by the Spanish "Ministerio de Economía y Competitividad" (MINECO). Additional support for mineral microanalysis was provided by the Ramón y Cajal Fellowships RYC-2012-11314 and RYC-2015-17596, and by the Project CGL2016-81085 granted by the MINECO. LA-MC-ICPMS used for analysis of U-Pb and Lu-Hf isotopes on zircons at University of Chile was funded by FONDAP project no. 15090013 "*Centro de Excelencia en Geotermia de los Andes, CEGA*". This is also a contribution from the ARC National Key Centre for Geochemical Evolution and Metallogeny of Continents (www.es.mq.edu.au/GEMOC) and the ARC Centre of Excellence for Core to Crust Fluid Systems. SHRIMP facility and technical staff at Curtin University are also thanked for their support on the data acquisition.

Appendix A. Supplementary data

Supplementary data associated with this article can be found, in the online version, at http://dx.doi.org/10.1016/j.oregeorev.2017.02.012.

References

Acosta, A., 1997. Estudio de los fenómenos de fusión cortical y generación de granitoides asociados a las peridotitas de Ronda (Unpublished PhD. Thesis). Univ. Granada.

Acosta, A., Pereira, M.D., Shaw, D.M., Bea, F., 1997. Serpentinización de la peridotita de Ronda (Cordillera Bética) por la interacción con fluidos ricos en volátiles: comportamiento del B. Rev. Soc. Geol. España 10 (3–4), 301–308.

Acosta-Vigil, A., Rubatto, D., Bartoli, O., Cesare, B., Meli, S., Pedrera, A., Azor, A., Tajčmanová, L., 2014. Age of anatexis in the crustal footwall of the Ronda peridotites, S Spain. Lithos 210–211, 147–167. http://dx.doi.org/10.1016/j.lithos.2014.08.018.

Akbulut, M., González-Jiménez, J.M., Griffin, W.L., Belousova, E., O'Reilly, S.Y., McGowan, N., Pearson, N.J., 2016. Tracing ancient events in the lithospheric mantle: a case study from ophiolitic chromitites of SW Turkey. J. A. Earth Sci. 119, 1–19.

Balanyá, J.C., García Dueñas, V., Azañon, J.M., Sánchez Gómez, M., 1997. Alternating contractional and extensional events in the Alpujarride Nappes of the Alboran domain (Betics, Gibraltar arc). Tectonics 16, 226–238.

Ballhaus, C., 1998. Origin of podiform chromite deposits by magma mingling. Earth. Planet. Sci. Lett. 156, 185–193.

Bea, F., Fershtater, G.B., Montero, P., Whitehouse, M., Levi, V.Y., Scarrow, J.H., Austrheim, H., Pushkariev, E.V., 2001. Recycling of continental crust into the mantle as revealed by Kytlym dunite zircons, Ural Mts, Russia. Terranova 13, 407–412.

Bédard, J.H., Hébert, R., 1998. Formation of chromitites by assimilation of crustal pyroxenites and gabbros into peridotitic intrusions: North Arm Mountain massif, Bay of Islands ophiolite, Newfoundland. Canada. J. Geophy. Research 103, 5165–5184.

Belousova, E.A., Griffin, W.L., O'Reilly, S.Y., Fisher, N.I., 2002. Igneous zircon: trace element composition as an indicator of source rock type. Contrib. Mineral. Petrol. 143, 602–622.

Belousova, E.A., Reid, A.J., Griffin, W.L., O'Reilly, S.Y., 2009. Rejuvenation vs. recycling of archean crust in the Gawler Craton, South Australia. Evidence from U-Pb and Hf- isotopes in Detrital Zircon. Lithos 113, 570–582.

Belousova, E.A., Kostitsyn, Y.A., Griffin, W.L., Begg, G.C., O'Reilly, S.Y., Pearson, N.J., 2010. The growth of the continental crust: constraints from zircón Hf-isotope data. Lithos 119, 457–466.

Belousova, E., González-Jiménez, J.M., Graham, I., Griffin, W.L., O'Reilly, S.Y., Pearson, N.J., Martin, L., Craven, S., Talavera, C., 2015. The enigma of crustal zircons in upper mantle rocks: clues from the Coolac ophiolite, SE Australia. Geology 43 (2), 119–122. http://dx.doi.org/10.1130/G36231.1.

Berly, T.J., Hermann, J., Arculus, R.J., Lapierre, H., 2006. Supra-subduction zone pyroxenites from San Jorge and Santa Isabel (Solomon Islands). J. Petrol. 47, 1531–1555.

Bodinier, J.L., Garrido, C.J., Chanefo, I., Bruguier, O., Gervilla, F., 2008. Origin of pyroxenite–pe- ridotite veined mantle by refertilization reactions: evidence from the Ronda peridotite (Southern Spain). J. Petrol. 49, 999–1025.

Booth-Rea, G., Ranero, C.R., Martinez-Martinez, J.M., Grevemeyer, I., 2007. Crustal types and Tertiary tectonic evolution of the Alboran sea, western Mediterranean. Geochem. Geophys. Geosyst. 8, 25.

Cavosie, A.J., Valley, J.W., Wilde, S.A., 2007. The oldest terrestrial mineral record: a review of 4400 to 3900 Ma detrital zircons from Jack Hills, Western Australia. In: Van Kranendonk, M.J., Smithies, R.H., Bennett, V. (Eds.), Earth's Oldest Rocks, Developments in Precambrian Geology. Elsevier, Amsterdam, pp. 91–111.

Condie, K.C., Aster, R.C., 2009. Zircon age episodicity and growth of continental crust. Eos Trans. AGU 90 (41). http://dx.doi.org/10.1029/2009EO410003. 364–364.

Crespo, E., Luque, F.J., Rodas, M., Wada, H., Gervilla, F., 2006. Graphite-sulfide deposits in Ronda and Beni Bousera peridotites (Spain and Morocco) and the origin of carbon in mantle-derived rocks. Gondwana Res. 9, 279–290.

Cuevas, J., Esteban, J.J., Tubía, J.M., 2006. Tectonic implications of the granite dyke swarm in the Ronda peridotites (Betic Cordilleras, Southern Spain). J. Geol. Soc. London 163, 631–640.

Davies, G.R., Nixon, P.H., Pearson, D.G., Obata, M., 1993. Tectonic implications of graphitized diamonds from the Ronda, peridotite massif, southern Spain. Geology 21, 471–474.

Downes, H., 2007. Origin and significance of spinel and garnet pyroxenites in the shallow lithospheric mantle: ultramafic massifs in orogenic belts in Western Europe and NW Africa. Lithos 99, 1–24.

Edwards, S.J., Pearce, J.A., Freeman, J., 2000. New insights concerning the influence of water during the formation of podiform chromite. Boulder. In: Dilek, Y., Moores, E.M., Elthon, D., Nicolas, A. (Eds.), Ophiolites and Oceanic Crust: New Insights from Field Studies and the Ocean Drilling Program. Geological Society of America, pp. 139–147. Special Paper 349.

Esteban, J.J., Sánchez-Rodríguez, L., Seward, D., Cuevas, J., Tubía, J.M., 2004. The late thermal history of the Ronda area, southern Spain. Tectonophysics 389, 81–92.

Esteban, J.J., Cuevas, J., Tubía, J.M., Liati, A., Seward, D., Gebauer, D., 2007. Timing and origin of zircon-bearing chlorite schists in the Ronda peridotites (Betic Cordilleras, Southern Spain). Lithos 99, 121–135.

Esteban, J.J., Cuevas, J., Tubía, J.M., Sergeev, S., Larionov, A., 2010. A revised aquitanian age for the emplacement of the Ronda peridotites (Betic Cordilleras, Southern Spain). Geol. Mag. 148, 183–187.

Esteban, J.J., Tubía, J.M., Cuevas, J., Vegas, N., Sergeev, S., Larionov, A., 2011. Peri-Gondwanan provenance of pre-Triassic metamorphic sequences in the western Alpujarride nappes (Betic Cordillera, southern Spain). Gondwana Res. 20, 443–449. http://dx.doi.org/10.1016/j.gr.2010.11.006.

Faccenna, C., Piromallo, C., Crespo-Blanc, A., Jolivet, L., Rossetti, F., 2004. Lateral slab deformation and the origin of the western Mediterranean arcs. Tectonics 23, 12. http://dx.doi.org/10.1029/2002TC001488. TC1012.

Garrido, C.J., Bodinier, J.L., 1999. Diversity of mafic rocks in the Ronda peridotite: evidence for pervasive melt-rock reaction during heating of subcontinental lithosphere by upwelling asthenosphere. J. Petrol. 40, 729–754.

Garrido, C.J., Gueydan, F., Booth-Rea, G., Precigout, J., Hidas, K., Padron-Navarta, J.A., Marchesi, C., 2011. Garnet lherzolite and garnet-spinel mylonite in the Ronda peridotite: vestiges of Oligocene backarc mantle lithospheric extension in the western Mediterranean. Geology 39, 927–930. http://dx.doi.org/10.1130/G31760.1.

Gebauer, D., 1996. A P-T-t path for a (ultra?-) high pressure ultramafic/mafic rock-associations and their felsic country- rocks based on SHRIMP-dating of magmatic and metamorphic zircon domains. Example: Alpe Arami (Central Swiss Alps). In: Basu, A., Hart, S. (Eds.), Earth processes: reading the isotopic code, Geophysical Monographs. AGU, Washington, DC, pp. 307–329.

Gervilla, F., 1990. Mineralizaciones Magmáticas Ligadas a La Evolución De Las Rocas Ultramáficas De La Serranía De Ronda (Málaga–España). Universidad de Granada, Granada, p. 189.

Gervilla, F., Leblanc, M., 1990. Magmatic ores in high temperature alpine-type Lherzolite massifs (Ronda, Spain, and Beni Bousera, Morocco). Econ. Geol. 85, 112–132.

Gervilla, F., Leblanc, M., Torres-Ruiz, J., Fenoll Hach-Alí, P., 1996. Immiscibility between arsenide and sulfide melts: a mechanism for the concentration of noble metals. Can. Mineral. 34, 485–502.

Gervilla, F., Gutiérrez-Narbona, R..Fenoll., Hach-Alí, P., 1999. Genesis of small chromitite bodies at the later stages of melt/rock interaction in the Ojén ultramafic massif, south Spain. In: Stanley, C.J. et al. (Eds.), Mineral Deposits: Processes to Processing. Balkema, Rotterdam, SGA London, pp. 725–728.

Gervilla, F., Cabri, L.J., Kojonen, K., Sie, S.H., Papunen, H., Fenoll Hach-Alí, P., 2000. Trace platinum-group elements in arsenide and sulfarsenides from magmatic ores: an electron microprobe and proton microprobe (micro-PIXE technique) study. Cuadernos del Laboratorio Geológico de Laxe 25, 103–105.

Gervilla, F., Cabri, L.J., Kojonen, K., Oberthür, T., Weiser, T.W., Johanson, B., Sie, S.S., Campbell, J.L., Teesdale, W.J., Laflame, J.H.G., 2004. Platinum-group element distribution in some ore deposits: results of EPMA and Micro-PIXE analyses. Microchim. Acta 147, 167–173.

Giuliani, G., Fallick, A., Rakotondrazafy, M., Ohnenstetter, D., Andriamamonjy, A., Ralantoarison, T., Rakotosamizanany, S., Razanatseheno, M., Offant, Y., Garnier, V., Dunaigre, C., Schwarz, D., Mercier, A., Ratrimo, V., Ralison, B., 2007. Oxygen isotope systematics of gem corundum deposits in Madagascar: relevance for their geological origin. Miner. Deposita. 42 (3), 251–270.

González-Jiménez, J.M., Villaseca, C., Griffin, W.L., Belousova, E., Conc, Z., Ancochea, E., O'Reilly, S.Y., Pearson, N., Garrido, C.J., Gervilla, F., 2013. The architecture of the European-Mediterranean Lithosphere: a synthesis of the Re-Os evidence. Geology 41, 547–550. http://dx.doi.org/10.1130/G34003.1.

González-Jiménez, J.M., Marchesi, C., Griffin, W.L., Gutiérrez-Narbona, R., Lorand, Jean, -P, O'Reilly, S.Y., Garrido, C.J., Gervilla, F., Pearson, N.J., Hidas, K., 2013. Transfer of Os isotopic signatures from peridotite to chromitite in the subcontinental mantle: insights from in situ analysis of platinum-group and base-metal minerals (Ojén peridotite massif, southern Spain). Lithos 164–167, 74–85. http://dx.doi.org/10.1016/j.lithos.2012.07.009.

González-Jiménez, J.M., Griffin, W.L., Proenza, J.A., Gervilla, F., O'Reilly, S.Y., Akbulut, M., Pearson, N.J., Arai, S., 2014. Chromitites in ophiolites: How, where, when, why? Part II. The crystallization of chromitites. Lithos 189, 140–158. http://dx.doi.org/10.1016/j.lithos.2013.09.008.

González-Jiménez, J.M., Locmelis, M., Belousova, E., Griffin, William L., Gervilla, F., Kerestedjian, T., O'Reilly, S.Y., Sergeeva, I., Pearson, N.J., 2015. Genesis and tectonic implications of podiform chromitites in the metamorphosed Ultramafic Massif of Dobromirtsi (Bulgaria). Gondwana Res. 27, 555–574.

Grant, T.B., Harlov, D.E., Rhede, D., 2016. Experimental formation of pyroxenite veins by reactions between olivine and Si, Al, Ca, Na, and Cl-rich fluids at 800 °C and 800 MPa: implications for fluid metasomatism in the mantle wedge. Am. Mineral. 101 (4), 808–818. http://dx.doi.org/10.2138/am-2016-5441.

Grieco, G., Ferrario, A., Von Quadt, A., Koeppel, V., Mathez, E.A., 2001. The zircon-bearing chromitites of the phlogopite peridotite of Finero (Ivrea zone, southern Alps): evidence and geochronology of a metasomatized mantle slab. J. Petrol. 42 (1), 89–101.

Griffin, W.L., Wang, X., Jackson, S.E., Pearson, N.J., O'Reilly, S.Y., Xu, X., Zhou, X., 2002. Zircon chemistry and magma genesis, SE China: in-situ analysis of Hf isotopes, Tonglu and Pingtan Igneous Complexes. Lithos 61 (3), 237–269.

Griffin, W.L., Belousova, E.A., Shee, S.R., Pearson, N.J., O'Reilly, S.Y., 2004. Archean crustal evolution in the northern Yilgarn Craton: U-Pb and Hf-isotope evidence from detrital zircons. Precamb. Res. 13, 231–282.

Griffin, W.L., Yang, J., Robinson, P.T., Howell, D., O'Reilly, S.Y., Pearson, N., 2013. Going up or going down? Diamonds and super-reducing UHP assemblages in ophiolitic mantle. Mineral. Mag. 77, 1215.

Griffin, W.L., Afonso, J.C., Belousova, E.A., Gain, S.E., Gong, X.H., González-Jiménez, J. M., Howell, D., Huang, J.X., McGowan, N., Pearson, N.J., Satsukawa, T., Shi, R., Williams, P., Xiong, Q., Yang, J.S., Zhang, M., O'Reilly, S.Y., 2016. Mantle recycling: transition zone metamorphism of Tibetan ophiolitic peridotites and its tectonit implications. J. Petrol. 57, 655–684.

Gutierrez-Narbona, R., Lorand, J.-P., Gervilla, F., Gros, M., 2003. New data on base-metal mineralogy and platinum-group minerals in the Ojen chromitites (Serranía de Ronda, Betic Cordillera, southern Spain). Neues Jahrbuch für Mineralogie – Abhandlungen 179, 143–173.

Gutiérrez-Narbona, R., 1999. Implicaciones metalogénicas (cromo y elementos del grupo del platino) de los magmas/fluidos residuales de un procesos de precolacióna gran escala en los macizos ultramáficos de Ronda y Ojén (Béticas, sur de España). Tesis Univ, Granada, p. 292.

Harrison, T.M., 2009. The hadean crust: evidence from >4 Ga Zircons. Annu. Rev. Earth Planet. Sci. 37, 479–505.

Hermann, J., Rubatto, D., Trommsdorff, V., 2006. Subsolidus Oligocene zircon formation in garnet peridotite during fast decompression and fluid infiltration (Duria, Central Alps). Mineral. Petrol. 88, 181–206.

Hernández-Pacheco, A., 1967. Estudio petrográfico y geoquimico del macizo ultramáfico de Ojéne (Málaga), 23. Inst "Lucas Mallada" Estudio Geológicos. 85-143.

Hidas, K., Booth-Rea, G., Garrido, C.J., Martínez-Martínez, J.M., Padrón-Navarta, J.A., Konc, Z., Giaconia, F., Frets, E., Marchesi, C., 2013. Backarc basin inversion and subcontinental mantle emplacement in the crust: kilometre-scale folding and shearing at the base of the proto-Alborán lithospheric mantle (Betic Cordillera, southern Spain). J. Geol. Soc. 170, 47–55. http://dx.doi.org/10.1144/jgs2011-151.

Hidas, K., Varas-Reus, M.I., Garrido, C.J., Marchesi, C., Acosta-Vigil, A., Padrón-Navarta, J.A., Targuisti, K., Konc, Z., 2015. Hyperextension of continental to oceanic-like lithosphere: The record of late gabbros in the shallow subcontinental lithospheric mantle of the westernmost Mediterranean. Tectonophysics 650, 65–79. http://dx.doi.org/10.1016/j.tecto.2015.03.011.

Hill, R., Roeder, P.L., 1974. The crystallization of spinel from basaltic liquid as a function of oxygen fugacity. J. Geol. 82, 709–729.

Hoskin, P.W.O., Schaltegger, U., 2003. The composition of zircon and igneous and metamorphic petrogenesis. Rev. Mineral. Geochem. 53, 27–62.

Irvine, T.N., 1975. Crystallization sequences in the Muskox intrusion and other layered intrusions-II. Origin of chromitite layers and similar deposits of other magmatic ores. Geochim. Cosmochim. Acta 39, 991–1020.

Kinny, P.D., Maas, R., 2003. Lu-Hf and Sm-Nd isotope systems in zircon. In: Hanchar, J.M., Hoskin, P. W. O (Eds.), Zircon. Reviews in Mineralogy and Geochemistry, 53, pp. 327–341.

Lambart, S., Laporte, D., Schiano, O., 2009. An experimental study of focused magma transport and basalt–peridotite interactions beneath mid-ocean ridges: implications for the generation of primitive MORB compositions. Contrib. Mineral. Petrol. 157, 429–451.

Leblanc, M., Gervilla, F., Jedwab, J., 1990. Noble metals segregations and fractionation in magmatic ores from Ronda and Beni Bousera Lherzolite massifs (Spain, Morocco). Mineral. Petrol. 42, 233–248.

Lenoir, X., Garrido, C.J., Bodinier, J.-L., Dautria, J.M., Gervilla, F., 2001. The recrystallization front of the Ronda peridotite: evidence for melting and thermal erosion of subcontinental lithospheric mantle beneath the Alboran Basin. J. Petrol. 42, 141–158.

Li, H.-Y., Chen, R.-X., Zheng, Y.-F., Hu, Z., 2016. The crust-mantle interaction in continental subduction channels: Zircon evidence from orogenic peridotite in the Sulu orogen. J. Geophys. Res. Solid Earth. 121, 687–712. http://dx.doi.org/10.1002/ 2015JB012231.

Liati, A., Gebauer, D., 2009. Crustal origin of zircon in a garnet peridotite: a study of U-Pb SHRIMP dating, mineral inclusions and REE geochemistry (Erzgebirge, Bohemian Massif). Eur. J. Mineral. 21, 737–750. http://dx.doi.org/10.1127/0935-1221/2009/0021-1939.

Liu, L.-G., 1979. High-pressure phase transformations in baddeleyite and zircon, with geophysical implications. Earth Planet. Sci. Lett. 44, 390–396.

Liou, J.G., Tsujimori, T., 2013. The fate of subducted continental crust: Evidence from recycled UHP-UHT minerals. Elements 9, 248–250.

Liu, Y.S., Gao, S., Hu, Z.C., Gao, C.G., Zong, K.Q., Wang, D., 2010. Continental and oceanic crust recycling-induced melt-peridotite interactions in the Trans-North China Orogen: U-Pb dating, Hf isotopes and trace elements in zircons from mantle xenoliths. J. Petrol. 51, 537–571. http://dx.doi.org/10.1093/petrology/egp082.

Lorand, J.-P., 1983. Les mineraux opaques des lherzolites à spinell et des pyroxénites associées Thèse 3ème Cycle. Université de Paris VI. 258 p..

Manning, C.E., 2004. The chemistry of subduction zone fluids. Earth Planet. Sci. Lett. 223, 1–16.

Marchesi, C., Griffin, W.L., Garrido, C.J., Bodinier, J.-L., O'Reilly, S.Y., Pearson, N.J., 2010. Persistence of mantle lithospheric Re–Os signature during asthenospherization of the subcontinental lithospheric mantle: insights from in situ isotopic analysis of sulfides from the Ronda peridotite (southern Spain). Contrib. Mineral. Petrol. 159, 315–330.

Marchesi, C., Garrido, C.J., Bosch, D., Bodinier, J.-L., Hidas, K., Padrón-Navarta, J.A., Gervilla, F., 2012. A late oligocene suprasubduction setting in the westernmost mediterranean revealed by intrusive pyroxenite dikes in the ronda peridotite (Southern Spain). J. Geol. 120, 237–247.

Marchesi, C., Garrido, C.J., Bosch, D., Bodinier, J.-L., Gervilla, F., Hidas, K., 2013. Mantle refertilization by melts of crustal-derived garnet pyroxenite: evidence from the Ronda peridotite massif, southern Spain. Earth Planet. Sci. Lett. 362, 66–75.

Marchesi, C., Dale, C.W., Garrido, C.J., Pearson, D.G., Bosch, D., Bodinier, J.-L., Gervilla, F., Hidas, K., 2014. Fractionation of highly siderophile elements in refertilized mantle: implications for the Os isotope composition of basalts. Earth Planet. Sci. Lett. 400, 33–44.

Marchi, S., Bottke, W.F., Elkins-Tanton, L.T., Bierhaus, M., Wuennemann, K., Mordibelli, A., Kring, D.A., 2014. Widespread mixing and burial of Earth's Hadean crust by asteroid impacts. Nature 511, 578–582.

McGowan, N.M., Griffin, W.L., González-Jiménez, J.M., Belousova, E.A., Afonso, J., Shi, R., McCammon, C.A., Pearson, N.J., O'Reilly, S.Y., 2015. Tibetan chromitites: excavating the slab graveyard. Geology 43, 179–182.

Monié, P., Torres-Roldán, R.L., García-Casco, A., 1994. Cooling and exhumation of the Western Betic Cordilleras, $^{40}Ar/^{39}Ar$ thermochronological constraints on a collapsed terrane. Tectonophysics 238, 353–379.

Morishita, T., Arai, S., Gervilla, F., 2001. High-pressure aluminous mafic rocks from the Ronda Peridotite massif, Southern Spain: significance of sapphirine- and corundum- bearing mineral assemblages. Lithos 57, 143–161.

Morishita, T., Arai, S., Gervilla, F., Green, D.H., 2003. Closed-system recycling of crustal materials in the alpine- type peridotite. Geochim. Cosmochim. Acta 67, 303–310.

Morishita, T., Arai, S., Ishida, Y., Tamura, A., Gervilla, F., 2009. Constraints on the evolutionary history of aluminous mafic rocks in the Ronda peridotite massif (Spain) from trace-element compositions of clinopyroxene and garnet. Geochem. J. 43, 191–206.

Navarro-Vilá, F., Tubía, J.M., 1983. Essai d'une nouvelle differentiation des Nappes Alpujarrides dans le secteur occidental des Cordillères Bétiques (Andalousie, Espagne). Comptes Rendus de la Academie des Sciences, Paris 296, 111–114.

Obata, M., 1980. The Ronda Peridotite: Garnet-, Spinel-, and Plagioclase-Lherzolite Facies and the P-T trajectories of a high-temperature mantle intrusion. J. Petrol. 21, 533–572.

Oen, I.S., 1973. A peculiar type of Cr-Ni-mineralization; cordierite-chromite-niccolite ores of Málaga, Spain, and their possible origin by liquid unmixing. Econ. Geol. 68, 831–842.

Oen, I.S., Kieft, C., Westerhof, A.B., 1973. Composition of chromites in cordierite- and mica-bearing Cr-Ni- ores from Málaga province, Spain. Mineral. Mag. 39, 193–203.

Ono, S., Funakoshi, K., Nakajima, Y., Tange, Y., Katsura, T., 2003. Geology Fields. Okoyama University, pp. 1–22.

Pearson, D.G., Davies, G.R., Nixon, P.H., Milledge, H.J., 1989. Graphitized diamonds from a peridotite massif in Morocco and implications for anomalous diamond occurrences. Nature 338, 60–62.

Pereira, M.D., Shaw, D.M., Acosta, A., 2003. Mobile trace elements and fluid-dominated processes in the Ronda peridotite, Southern Spain. Can. Mineral. 41, 617–625.

Piña, R., Gervilla, F., Barnes, S.-J., Ortega, L., Lunar, R., 2013. Partition coefficients of platinum-group and chalcophile elements between arsenide and sulfphide phases as determined in the Beni Bousera Cr-Ni mineralization (North Morocco). Econ. Geol. 108, 935–951.

Piña, R., Gervilla, F., Barnes, S.-J., Ortega, L., Lunar, R., 2015. Liquid immiscibility between arsenide and sulfide melts: Evidence from a LA-ICP-MS study in magmatic deposits at Serranía de Ronda (Spain). Miner. Deposita 50, 265–279.

Platt, J.P., Soto, J.I., Whitehouse, M.J., Hurford, A.J., Kelley, S.P., 1998. Thermal evolution, rate of exhumation, and tectonic significance of metamorphic rocks from the floor of the Alboran extensional basin, western Mediterranean. Tectonics 17, 671–689.

Platt, J.P., Behr, W.M., Johanesen, K., Williams, J.R., 2013. The betic-rif arc and its orogenic hinterland: a review. Annu. Rev. Earth Planet. Sci. 41, 313–357. http://dx.doi.org/10.1146/annurev-earth-050212-123951.

Precigout, J., Gueydan, F., Gapais, D., Garrido, C.J., Essaifi, A., 2007. Strain localisation in the subcontinental mantle - a ductile alternative to the brittle mantle. Tectonophysics 445, 318–336. http://dx.doi.org/10.1016/j.tecto.2007.09.002.

Priem, H.N.A., Boelrijk, N.A.I.M., Hebeda, E.H., Oen, I.S., Verdurmen, E.A.Th., Verschure, R.H., 1979. Isotopic dating of the emplacement of the ultramafic masses in the Serrania de Ronda, Southern Spain. Contrib. Mineral. Petrol. 70, 103–109.

Prouteau, G., Scaillet, B., Pichavant, M., Maury, R., 2001. Evidence for mantle metasomatism by hydrous silicic melts derived from subducted oceanic crust. Nature 410, 197–200.

Rapela, C.W., Baldo, E.G., Pankhurst, R.J., Saavedra, J., 2002. Cordieritite and leucogranite formation during emplacement of highly peraluminous magma: The El Pilon granite complex (Sierras Pampeanas, Argentina). J. Petrol. 43 (6), 1003–1028.

Reid, A.F., Ringwood, A.E., 1969. Newly observed high-pres- sure transformations in Mn_3O_4, $CaAl_2O_4$ and $ZrSiO_4$. Earth Planet. Sci. Lett. 6, 205–214.

Reisberg, L., Lorand, J.-P., 1995. Longevity of sub-continental mantle lithosphere from osmium isotope systematics in orogenic peridotite massifs. Nature 376, 159–162.

Robinson, P.T., Trumbull, R.B., Schmitt, A., Yang, J.S., Li, J.W., Zhou, M.F., Erzinger, J., Dare, S., Xiong, F., 2015. The origin and significance of crustal minerals in ophiolitic chromitites and peridotites. Gondwana Res. 27, 486–506. http://dx.doi.org/10.1016/j.gr.2014.06.003.

Sánchez-Rodríguez, L., Gebauer, D., Tubía, J.M..Gil., Ibarguchi, J.I., Rubatto, D., 1996. First shrimp-ages on pyroxenites, eclogites and granites of the Ronda Complex and its country rocks. Geogaceta 20, 487–488.

Sánchez-Rodriguez, L., Gebauer, D., 2000. Mesozoic formation of pyroxenites and gabbros in the Ronda area (southern Spain), followed by Early Miocene subduction metamorphism and emplacement into the middle crust: U-Pb sensitive high- resolution ion microprobe dating of zircón. Tectonophysics 316 (1–2), 19–44.

Sen, G., Presnall, D.C., 1984. Liquidus phase relationships on the join anorthite-forsterite-quartz at 10 kbar with applications to basalt petrogenesis. Contrib. Mineral. Petrol. 85, 404–408.

Siebel, W., Schmitt, A.K., Daniski, M., Chen, F., Meier, S., Weiβ, S.E., Sümeyya, 2009. Prolonged mantle residence of zircon xenocrysts from the western Eger rift. Nat. Geosci. Lett. 2, 886–890. http://dx.doi.org/10.1038/NGEO695.

Thiéry, V., 2011. Cumulative cordieritite formation as a result of anatexis and melt expulsion. An example from the Chavanon sequence, Variscan French Massif Central. Periodico di Mineralogia 80 (2), 267–285. http://dx.doi.org/10.2451/2011 PM0020.

Torres-Ruiz, J., Garuti, G., Gazzotti, M., Gervilla, F., Fenoll Hach-Alí, P., 1996. Platinum- group minerals in chromitites from the Ojen lherzolite massif (Serranía de Ronda, Betic Cordillera, Southern Spain). Mineral. Petrol. 56, 25–50.

Tubía, J.M., 1985. Sucesiones metamórficas asociadas a ro- cas ultramáficas en los Alpujárrides occidentales (Cordilleras Béticas, Málaga) Tesis Doctoral. Univ. del País Vasco, p. 263.

Tubía, J.M., Cuevas, J., 1986. High-temperature emplacement of the Los Reales peridotite nappe (Betic Cordillera Spain). J. Struct. Geol. 8, 473–482.

Tubía, J.M., Cuevas, J., Gil Ibarguchi, J.I., 1997. Sequential development of the metamorphic aureole beneath the Ronda peridotites and its bearing on the tectonic evolution of the Betic Cordillera. Tectonophysics 279, 225–227.

Valley, J.W., Kinny, P.D., Schulze, D.J., Spicuzza, M.J., 1998. Zircon megacrysts from kimberlite: oxygen isotope variability among mantle melts. Contrib. Mineral. Petrol. 133, 1–11. http://dx.doi.org/10.1007/s004100050432.

Valley, J.W., 2003. Oxygen isotopes in zircon. In: Hanchar, J.M., Hoskin, P.W.O. (Eds.), Zircon. Reviews in Mineralogy and Geochemistry, 53, pp. 343–385.

Valley, J.W., Lackey, J.S., Cavosie, A.J., Clechenko, C.C., Spicuzza, M.J., Basei, M.A.S., Bindeman, I.N., Ferreira, V.P., Sial, A.N., King, E.M., Peck, W.H., Sinha, A.K., Wei, C. S., 2005. 4.4 billion years of crustal maturation: oxygen isotopes in magmatic zircon. Contrib. Mineral. Petrol. 150, 561–580. http://dx.doi.org/10.1007/s00410-005-0025-8.

Van der Wal, D., Bodinier, J.-L., 1996. Origin of the recrystallisation front in the Ronda peridotite by km-scale pervasive porous melt flow. Contrib. Mineral. Petrol. 122, 387–405.

Van der Wal, D., Vissers, R.L.M., 1993. Uplift and emplacement of upper mantle rocks in the western Mediterranean. Geology 21, 1119–1122. http://dx.doi.org/10.1130/0091- 7613(1993) 021∗1119:uaeoum∗2.3.co; 2.

Van der Wal, D., Vissers, R.L.M., 1996. Structural petrology of the Ronda Peridotite, SW Spain: deformation history. J. Petrol. 37, 23–43.

Varas-Reus, M.I., Garrido, C.J., Marchesi, C., Bosch, D., Acosta-Vigil, A., Hidas, K., Barich, A., Booth-Rea, G., 2016. Sr-Nd-Pb-Hf isotopic systematics of crustal rocks from the western Betics (S Spain): Implications for crustal recycling in the lithospheric mantle beneath the westernmost Mediterranean. Lithos. http://dx.doi.org/10.1016/j.lithos.2016.10.003.

Xiong, F., Yang, J., Robinson, P.T., Xu, X., Liu, Z., Li, Y., Li, J., Chen, S., 2015. Origin of podiform chromitite, a new model base don the Luobusa ophiolite, Tibet. Gondwana Res. 27, 525–542.

Xu, X., Yang, J., Robinson, P., Xiong, F., Ba, D., Guo, G., 2015. Origin of ultrahigh pressure and highly reduced minerals in podiform chromitites and associated peridotites of the Luobusa ophiolite. Tibet. Gondwana Res. 27, 686–700.

Yamamoto, S., Komiya, T., Hirose, K., Maruyama, S., 2003. Zircons from chromitite in Luobusa ophiolite, Tibet. Godlschmidt Conference Abstracts, p. A553 (abstract).

Yamamoto, S., Komiya, T., Hirose, K., Maruyama, S., 2004. Crustal zircons from the podiform chromitites in Luobusa ophiolite, Tibet. American Geophysical Union. Fall Meeting 2004 (abstract V31C-1443).

Yamamoto, S., Komiya, T., Yamamoto, H., Kaneko, Y., Terabayashi, M., Katayama, I., Iizuka, T., Maruyama, S., Yang, J., Kon, Y., Hirata, T., 2013. Recycled crustal zircons from podiform chromitites in the Luobusa ophiolite, southern Tibet. The Island Arc 22, 89–103.

Yaxley, G.M., Green, D.H., 1998. Reactions between eclogite and peridotite: mantle refertilisation by subduction of oceanic crust. Schwetz Mineral Petrogr. Mitt. 78, 243–255.

Zeck, H.P., Albat, F., Hansen, B.T., Torres-Roldan, R.L., García-Casco, A., Martín-Algarra, A., 1989. A 21± 2 Ma age for the termination of the ductile Alpine deformation in the internal zone of the Betic Cordilleras, south Spain. Tectonophysics 169, 215–220.

Zheng, J., Griffin, W.L., O'Reilly, S.Y., Zhang, M., Pearson, N., 2006. Zircons in mantle xenoliths record the Triassic Yangtze-North China continental collision. Earth Planet. Sci. Lett. 247, 130–142.

Zheng, Y.-F., 2012. Metamorphic chemical geodynamics in continental subduction zones. Chem. Geol. 328, 5–48. http://dx.doi.org/10.1016/j.chemgeo.2012.02.005.

Zhou, M.F., Robinson, P.T., Su, B.-X., Gao, J.-F., Li, J.-W., Yang, J.-S., Malpas, J., 2014. Com- positions of chromite, associated minerals, and parental magmas of podiform chromite deposits. The role of slab contamination of astheno- spheric melts in suprasubduction zone environ- ments. Gondwana Res. 26, 262–283. http://dx.doi.org/10.1016/j.gr.2013.12.011.

Zindler, A., Staudigel, H., Hart, S.R., Endres, R., Goldstein, S., 1983. Nd and Sr isotopic study of a mafic layer from Ronda ultramafic complex. Nature 304, 226–227.